

AD\_\_\_\_\_

Award Number: DAMD17-03-1-0263

TITLE: Targeted Ablation of CML Stem Cells

PRINCIPAL INVESTIGATOR: Craig T. Jordan, Ph.D.

CONTRACTING ORGANIZATION: University of Rochester  
Rochester, NY 14627-0140

REPORT DATE: January 2007

TYPE OF REPORT: Final

PREPARED FOR: U.S. Army Medical Research and Materiel Command  
Fort Detrick, Maryland 21702-5012

DISTRIBUTION STATEMENT: Approved for Public Release;  
Distribution Unlimited

The views, opinions and/or findings contained in this report are those of the author(s) and should not be construed as an official Department of the Army position, policy or decision unless so designated by other documentation.

REPORT DOCUMENTATION PAGE				Form Approved OMB No. 0704-0188	
Public reporting burden for this collection of information is estimated to average 1 hour per response, including the time for reviewing instructions, searching existing data sources, gathering and maintaining the data needed, and completing and reviewing this collection of information. Send comments regarding this burden estimate or any other aspect of this collection of information, including suggestions for reducing this burden to Department of Defense, Washington Headquarters Services, Directorate for Information Operations and Reports (0704-0188), 1215 Jefferson Davis Highway, Suite 1204, Arlington, VA 22202-4302. Respondents should be aware that notwithstanding any other provision of law, no person shall be subject to any penalty for failing to comply with a collection of information if it does not display a currently valid OMB control number. <b>PLEASE DO NOT RETURN YOUR FORM TO THE ABOVE ADDRESS.</b>					
1. REPORT DATE (DD-MM-YYYY) 01-01-2007		2. REPORT TYPE Final		3. DATES COVERED (From - To) 15 Apr 2003 – 14 Dec 2006	
4. TITLE AND SUBTITLE  Targeted Ablation of CML Stem Cells				5a. CONTRACT NUMBER	
				5b. GRANT NUMBER DAMD17-03-1-0263	
				5c. PROGRAM ELEMENT NUMBER	
6. AUTHOR(S)  Craig T. Jordan, Ph.D.  E-Mail: <a href="mailto:craig_jordan@urmc.rochester.edu">craig_jordan@urmc.rochester.edu</a>				5d. PROJECT NUMBER	
				5e. TASK NUMBER	
				5f. WORK UNIT NUMBER	
7. PERFORMING ORGANIZATION NAME(S) AND ADDRESS(ES)  University of Rochester Rochester, NY 14627-0140				8. PERFORMING ORGANIZATION REPORT NUMBER	
9. SPONSORING / MONITORING AGENCY NAME(S) AND ADDRESS(ES) U.S. Army Medical Research and Materiel Command Fort Detrick, Maryland 21702-5012				10. SPONSOR/MONITOR'S ACRONYM(S)	
				11. SPONSOR/MONITOR'S REPORT NUMBER(S)	
12. DISTRIBUTION / AVAILABILITY STATEMENT Approved for Public Release; Distribution Unlimited					
13. SUPPLEMENTARY NOTES					
14. ABSTRACT  This report summarizes progress and achievements for the grant entitled "Targeted ablation of CML stem cells". The work was initiated at the University of Kentucky in April of 2003, and transferred to the University of Rochester in December of 2003. The work was completed at the University of Rochester and encompasses studies using both mouse and human systems.					
15. SUBJECT TERMS No subject terms provided					
16. SECURITY CLASSIFICATION OF:			17. LIMITATION OF ABSTRACT	18. NUMBER OF PAGES	19a. NAME OF RESPONSIBLE PERSON
a. REPORT	b. ABSTRACT	c. THIS PAGE			USAMRMC
U	U	U	UU	64	19b. TELEPHONE NUMBER (include area code)

## Table of Contents

	<u>Page</u>
Introduction.....	4
Body.....	4
Key Research Accomplishments.....	4-5
Reportable Outcomes.....	5
Conclusion.....	5
References.....	6
Appendices.....	6

## Introduction

The human hematopoietic system is organized in a hierarchical fashion, with rare and specialized stem cells giving rise to all types of mature blood cells. Numerous studies have demonstrated that stem cells are absolutely essential to the blood formation process, and that diseases which affect stem cells are almost uniformly serious/life-threatening. Many previous studies have shown that chronic myelogenous leukemia (CML) is one such stem cell disease and that the clinical profile of CML is entirely consistent with stem cell dysfunction. Thus, in order to provide durable cures, it is clear that potential therapies must specifically target and destroy the CML stem cell.

Given the importance of stem cell targeting, the main objective of the proposed studies was to develop and characterize methods to ablate CML stem cells. Based on previous studies using AML stem cells, we hypothesized that CML stem cells can be induced to undergo apoptosis using clinically relevant drug regimens. Further, we proposed that CML-specific apoptosis can be achieved, while sparing normal stem cells. The specific aims of the study were: (1) To investigate apoptosis induction for human CML stem cells. (2) To analyze the role of NF- $\kappa$ B in survival of CML stem cells. (3) To investigate the in vivo biology of CML vs. normal stem cells in response to apoptotic stimuli using a mouse model system

## Body

Aim #1: The goal of investigation novel methods of apoptosis for leukemic stem cells was achieved and is described in appendices #1-2.

Aim #2: The goal of investigation the role of NF- $\kappa$ B in CML cells was achieved and is described in appendix #1-2.

Aim #3: The goal of developing and using a mouse model of CML stem cells was achieved and is described in appendix #3.

## Key Research Accomplishments

1. Developing a novel therapeutic agent for targeting leukemia stem cells:

The manuscripts provided in appendices #1 and #2 describe development of a novel drug for the treatment of leukemia. The agent is derived from the naturally-occurring compound parthenolide.

Studies in appendix #1 describe the activity of parthenolide and demonstrate that the agent is specifically cytotoxic to malignant stem cells derived from blast crisis CML patients. This exciting finding is the first demonstration of a drug that selective kills CML stem cells, while also sparing normal hematopoietic stem cells. The studies described in appendix #2 further develop clinical avenues by creating and testing a more pharmaceutically useful analog of parthenolide. Using both primary human specimens, as well as two in vivo models, the studies in appendix #2 demonstrate that our parthenolide analog is a promising agent for future clinical studies in CML.

## 2. Developing a novel mouse model of CML stem cells (appendix #3)

The second key research accomplishment from this work has been the development and utilization of a novel mouse model system for both chronic and blast crisis CML stem cells. In appendix #3 (now accepted for publication in *Blood*), we demonstrate that leukemic stem cells can be phenotypically identified, isolated, and characterized. The models are generated by retroviral transduction of normal hematopoietic stem/progenitor cells with the BCR/ABL and Nup98/HoxA9 translocations. By challenging leukemic animals with drug or radiation insults, we show that stem cell specific effects can only be ascertained by directly monitoring primitive populations. Indeed, relatively effects on bulk disease are often completely different than consequences observed for stem cells. Thus, the model provides a powerful means by which new therapeutic concepts may be studied with regard to leukemia stem cells in vivo.

## Reportable Outcomes

Appendices #1-3 (see below)

## Conclusions

The proposed goals of this project have been successfully completed.

“so what” section – the results obtained from this project are highly significant in two regards. First, the development a therapeutic agent that specifically targets CML stem cells is entirely novel and has direct ramifications for patient care. Second, the availability of a mouse model in which CML stem cells may be studied in vivo, provides new and exciting opportunities for drug development.

## References

N/A

## Appendices

### **Appendix #1:**

Guzman, M.L., Rossi, R.M., Karnischky, L., Li, X., Peterson, D., Howard, D.S., and Jordan, C.T. (2005). The sesquiterpene lactone parthenolide induces apoptosis of human acute myelogenous leukemia stem and progenitor cells. *Blood* – Plenary Paper, 105(11):4163-4169.

### **Appendix #2:**

Monica L. Guzman, Randall M. Rossi, Sundar Neelakantan, Xiaojie Li, Cheryl Corbett, Duane C. Hassane, Michael W. Becker, John M. Bennett, Edmund Sullivan, Joshua L. Lachowicz, Christopher J. Sweeney, William Matthews, Martin Carroll, Peter A. Crooks, and Craig T. Jordan (2007). An orally bioavailable parthenolide analog selectively eradicates acute myelogenous leukemia stem and progenitor cells. Submitted.

### **Appendix #3:**

Sarah J. Neering, Timothy Bushnell, Selcuk Sozer, John Ashton, Randall M. Rossi, Pin-Yi Wang, Deborah R. Bell, David Heinrich, Andrea Bottaro, and Craig T. Jordan (2007). Leukemia stem cells in a genetically defined murine model of blast crisis CML. *Blood*, in press.

# The sesquiterpene lactone parthenolide induces apoptosis of human acute myelogenous leukemia stem and progenitor cells

Monica L. Guzman, Randall M. Rossi, Lilliana Karnischky, Xiaojie Li, Derick R. Peterson, Dianna S. Howard, and Craig T. Jordan

Recent studies have described malignant stem cells as central to the initiation, growth, and potential relapse of acute and chronic myelogenous leukemia (AML and CML). Because of their important role in pathogenesis, rare and biologically distinct leukemia stem cells (LSCs) represent a critical target for therapeutic intervention. However, to date, very few agents have been shown to directly target the LSC population. The present studies demonstrate that parthenolide (PTL), a naturally occurring small molecule, induces

robust apoptosis in primary human AML cells and blast crisis CML (bcCML) cells while sparing normal hematopoietic cells. Furthermore, analysis of progenitor cells using in vitro colony assays, as well as stem cells using the nonobese diabetic/severe combined immunodeficient (NOD/SCID) xenograft model, show that PTL also preferentially targets AML progenitor and stem cell populations. Notably, in comparison to the standard chemotherapy drug cytosine arabinoside (Ara-C), PTL is much more specific to leukemia

cells. The molecular mechanism of PTL-mediated apoptosis is strongly associated with inhibition of nuclear factor  $\kappa$  B (NF- $\kappa$ B), proapoptotic activation of p53, and increased reactive oxygen species (ROS). On the basis of these findings, we propose that the activity of PTL triggers LSC-specific apoptosis and as such represents a potentially important new class of drugs for LSC-targeted therapy. (Blood. 2005;105:4163-4169)

© 2005 by The American Society of Hematology

## Introduction

Acute myelogenous leukemia (AML) is a malignant disease characterized by an aberrant accumulation of immature myeloid hematopoietic cells. Although remission can be achieved in most patients, relapse is common and long-term survival is poor for most cases. Studies using a variety of experimental systems have shown that AML arises from a rare population of leukemic stem cells (LSCs).<sup>1-3</sup> LSCs share some antigenic features with normal hematopoietic stem cells (HSCs), such as CD34<sup>+</sup>, CD38<sup>-</sup>, CD71<sup>-</sup>, and HLA-DR<sup>-</sup>, but can be phenotypically distinguished from HSCs by virtue of several disparate markers.<sup>1-6</sup> In addition, LSCs, like HSCs, are largely quiescent and display heterogeneity within the stem cell compartment.<sup>7-9</sup> As a consequence of these common features, it has been relatively difficult to define strategies to differentially target the LSC population. However, recent studies have demonstrated that LSCs do display certain unique molecular properties such as constitutive activation of nuclear factor  $\kappa$ B (NF- $\kappa$ B), expression of CD123, and potentially elevated levels of interferon regulatory factor 1 (IRF-1) and death-associated protein (DAP) kinase.<sup>6,8,10,11</sup> Features such as these suggest that LSC-specific targeted therapy should be feasible using a variety of strategies.

Current chemotherapy regimens for AML commonly use drugs such as nucleoside analogs (eg, cytosine arabinoside [Ara-C]) and anthracyclines (eg, idarubicin, daunorubicin) that interfere with DNA replication and induce apoptosis primarily in replicating

cells. Since LSCs are mostly quiescent, it is likely that at least some malignant stem cells are refractory to standard chemotherapy and may thereby contribute to relapse. Moreover, current regimens may not effectively discriminate between normal and malignant cells. Consequently, substantial damage to normal tissues is likely to occur in the course of standard treatments. For this reason, it is important to identify therapies that can specifically target the LSC population without affecting normal cells.

We have previously shown that a combination of the proteasome inhibitor MG-132 and the anthracycline idarubicin was sufficient to preferentially ablate human LSCs in vitro<sup>11</sup> while sparing normal hematopoietic cells. These studies demonstrate that LSC-specific targeting can be achieved. Interestingly, leukemia cell death was associated with inhibition of NF- $\kappa$ B and proapoptotic activation of p53. However, the overall toxicity of a proteasome inhibitor and an anthracycline to other tissues remains unknown. In addition, the cardiac toxicity of anthracyclines limits their use particularly in older individuals. Consequently, we have investigated other agents that may specifically ablate the LSC population.

Parthenolide (PTL) is a sesquiterpene lactone found as the major active component in Feverfew (*Tanacetum parthenium*), an herbal medicine that has been used to treat migraine and rheumatoid arthritis for centuries.<sup>12</sup> More recently, PTL has been found to have several other properties, including antitumor activity, inhibition of DNA synthesis, and inhibition of cell proliferation in different cancer cell lines.<sup>13-16</sup> In

From the University of Rochester School of Medicine, Division of Hematology/Oncology and Center of Human Genetics and Molecular Pediatric Disease and Department of Biostatistics and Computational Biology, Rochester, NY; and University of Kentucky Medical Center, Division of Hematology/Oncology, Lexington, KY.

Submitted October 28, 2004; accepted January 18, 2005. Prepublished online as *Blood* First Edition Paper, February 1, 2005; DOI 10.1182/blood-2004-10-4135.

Supported by grants from the National Institutes of Health (NIH; R01-CA90446) and the US Department of Defense (DAMD17-03-1-0263). C.T.J. is a scholar of

the Leukemia and Lymphoma Society.

An Inside *Blood* analysis of this article appears in the front of this issue.

**Reprints:** Monica L. Guzman, University of Rochester School of Medicine, 601 Elmwood Ave, Box 703, Rochester, NY 14642; e-mail: monica\_guzman@urmc.rochester.edu.

The publication costs of this article were defrayed in part by page charge payment. Therefore, and solely to indicate this fact, this article is hereby marked "advertisement" in accordance with 18 U.S.C. section 1734.

© 2005 by The American Society of Hematology

addition, PTL sensitizes cancer cells to other antitumor agents<sup>17-20</sup> and acts as a chemopreventive agent in a UVB-induced skin cancer animal model.<sup>21</sup> PTL is a potent inhibitor of NF- $\kappa$ B activation and has been shown to directly bind I $\kappa$ B-kinase (IKK)<sup>22,23</sup> and to modify the p50 and p65 NF- $\kappa$ B subunits.<sup>24,25</sup> PTL can also block signal transducers and activators of transcription 3 (STAT3) phosphorylation on Tyr705,<sup>26</sup> sustain c-Jun *N*-terminal kinase (JNK) activation,<sup>17,18</sup> and increase intracellular reactive oxygen species (ROS).<sup>13,27</sup> In this study, we analyzed the effect of PTL on survival of primary AML, blast crisis chronic myelogenous leukemia (bcCML), and normal hematopoietic cells. Our data demonstrate that PTL can selectively ablate primitive leukemia cells without affecting normal stem and progenitor cells. These findings indicate PTL and similar sesquiterpene lactones may represent a novel class of agents for targeting myeloid LSCs.

## Materials and methods

### Cell isolation and culture

AML cells, bcCML cells, normal bone marrow (BM), and umbilical cord blood (CB) cells were obtained from volunteer donors with informed consent or from the National Disease Research Interchange (NDRI). The cells were isolated and processed as described.<sup>6</sup> Briefly, samples were subjected to Ficoll-Paque (Pharmacia Biotech, Piscataway, NY) density gradient separation to isolate mononuclear cells. In some cases cells were cryopreserved in freezing medium consisting of Iscoves modified Dulbecco medium (IMDM), 40% fetal bovine serum (FBS), and 10% dimethylsulfoxide (DMSO). The viability of the leukemic cells after thawing was 50% to 95%. All the AML samples were 100% CD123<sup>+</sup>. The percent CD34 in the samples analyzed ranged from 20% to 80%. Fresh or thawed cells were cultured in serum-free medium (SFM)<sup>28</sup> for 1 hour before the addition of drugs. For PGJ2 (15-deoxy-delta12,14-prostaglandin J2; Cayman Chemical, Ann Arbor, MI) treatment, cells were cultured in the absence of bovine serum albumin (BSA). All the drug treatments were performed in triplicate. PTL (Biomol, Plymouth Meeting, PA) was reconstituted in DMSO to a stock concentration of 0.2 M and subsequently diluted in phosphate buffer saline (PBS). Ara-C was obtained from Sigma (St Louis, MO). Total cell numbers were determined before and after culture for several specimens. No significant nonspecific loss of cells was observed as a consequence of culture (data not shown).

### Methylcellulose colony-forming assay

AML or normal cells (BM or CB) were cultured in SFM as described in "Cell isolation and culture" for 18 hours in the presence or absence of drugs. Cells were then plated at 50 000 cells/mL in Methocult GF H4534 (1% methylcellulose in IMDM, 30% FBS, 1% BSA, 10<sup>-4</sup> M 2-mercaptoethanol, 2 mM L-glutamine, 50 ng/mL recombinant human [rh] stem cell factor, 10 ng/mL rh granulocyte-macrophage colony-stimulating factor [GM-CSF], 10 ng/mL rh interleukin 3 [IL-3]; Stem Cell Technologies, Vancouver, BC, Canada) supplemented with 3 units/mL of erythropoietin and 50 ng/mL G-CSF (R&D Systems, Minneapolis, MN). Colonies were scored after 10 to 14 days of culture.

### NOD/SCID mouse assays

Nonobese diabetic/severe combined immunodeficient (NOD/SCID; NOD.CB17-prdkdc scid/J) mice (Jackson Laboratories, Bar Harbor, ME) were sublethally irradiated with 2.7 Gy (270 rad) using a RadSource X-ray irradiator (RadSource, Boca Raton, FL) the day before transplantation. Cells to be assayed were injected via tail vein (5-10 million cells) in a final volume of 0.2 mL of PBS with 0.5% FBS. After 6 to 8 weeks, animals were killed and BM was analyzed for the presence of human cells by flow cytometry.

### EMSA and immunoblot analysis

Electrophoretic mobility shift assay (EMSA) was performed as described.<sup>8</sup> Briefly, nuclear extracts equivalent to 200 000 cells were incubated with 2  $\mu$ g of poly-d(I-C) (Roche Molecular Biochemicals, Indianapolis, IN) and 10<sup>-14</sup> mol <sup>32</sup>P-labeled NF- $\kappa$ B probe in 10 mM HEPES (*N*-2-hydroxyethylpiperazine-*N'*-2-ethanesulfonic acid), 5 mM Tris (tris(hydroxymethyl)aminomethane), 50 mM KCl, 1.2 mM EDTA (ethylenediaminetetraacetic acid), and 10% glycerol for 15 minutes at room temperature. Protein/DNA complexes were resolved on a native polyacrylamide gel in 0.25  $\times$  Tris-borate-EDTA (TBE). For immunoblots, cells were prepared and analyzed as previously described.<sup>6</sup> Blots were probed with anti-phospho-p53 (ser15), anti-phospho-PTEN (anti-phospho-phosphatase with tensin homology), anti-PTEN from Cell Signaling (Beverly, MA); anti-p53 (DO-1) from Santa Cruz Biotechnology (Santa Cruz, CA); and antiactin (AC-15) from Sigma.

### Flow cytometry

Apoptosis assays were performed as described.<sup>8</sup> Briefly, after 18 hours of treatment, specimens were labeled with anti-CD38-APC (anti-CD38-allophycocyanin) and anti-CD34-PE (anti-CD34-phycoerythrin; Becton Dickinson, San Jose, CA) for 20 minutes. Cells were then washed in cold PBS and resuspended in 200  $\mu$ L of annexin-V buffer. Annexin-V-fluorescein isothiocyanate (FITC) and 7-aminoactinomycin (7-AAD; Molecular Probes, Eugene, OR) were added and the samples were incubated at room temperature for 15 minutes followed by analysis using a Becton Dickinson LSRII flow cytometer. The total number of events collected ranged from 100 000 to 1 000 000, depending on the CD34<sup>+</sup>/CD38<sup>-</sup> content on the sample. The percent viable cells was defined as annexin-V<sup>-</sup>/7-AAD<sup>-</sup> cells on total (ungated) cells and on gates set for CD34<sup>+</sup> and CD34<sup>+</sup>/CD38<sup>-</sup> populations. To analyze human cell engraftment in the NOD/SCID xenogeneic model, BM cells were isolated, blocked with anti-Fc receptor antibody 2.4G2 and 25% human serum, and labeled with antihuman CD45, CD33, or CD19 antibodies (Becton Dickinson).

### Statistical analysis

We analyzed the data from CD34<sup>+</sup> and total cells separately by fitting separate linear mixed effects models to each dataset. We first log-transformed the percent viability measurements in order to reduce the influence of outliers and symmetrize the error distributions. Linear mixed effects models were then used to model the log (viability) as a function of the fixed effects for group (normal, AML, CML), dose (5.0, 7.5), and their interaction, along with a random intercept and dose effect for each subject to account for the correlation structure of the data. In addition, the residual variance was allowed to differ for each of the 3 groups (normal, AML, CML). Restricted maximum likelihood was used to estimate the parameters, and *P* values and 95% symmetric confidence intervals were computed using the robust "sandwich" estimator for standard errors on the logarithmic scale. Finally, the point estimates and confidence bounds were exponentiated back to the original scale of percent viability to obtain the estimated geometric means and fold changes along with their associated 95% asymmetric confidence intervals.

## Results

### PTL preferentially targets leukemia cells while sparing normal hematopoietic cells

Initial studies were performed to compare the effects of PTL on primary leukemia versus normal specimens during short-term suspension culture. The AML specimens represented different French-American-British (FAB) subtypes (Table 1) from both de novo and relapsed cases. Table 1 shows the effects of PTL treatment on AML, bcCML, and normal hematopoietic cells in both total and more primitive CD34<sup>+</sup> populations. Viability was

Table 1. Viability of leukemia and normal specimens in response to parthenolide

Specimens	FAB subtype	Cytogenetics	5 μM parthenolide				7.5 μM parthenolide			
			CD34 <sup>+</sup>		Total		CD34 <sup>+</sup>		Total	
			Average % viable*	SD	Average % viable*	SD	Average % viable*	SD	Average % viable*	SD
AML specimens										
AML1	M2	Probable 11q23	3.5	1.6	26.2	10.2	4.6	1.3	34.0	8.2
AML2	M4	Trisomy 8 and 13	6.0	3.3	18.2	3.4	10.6	6.4	22.2	9.6
AML3	M4 (AML2 relapse)	Trisomy 8 and 13	24.2	3.9	44.9	3.6	18.2	2.0	32.5	4.2
AML4	M4	Normal	4.9	1.0	30.9	1.6	4.3	0.3	24.9	1.5
AML5	M4 (AML4 relapse)	Normal	1.5	0.2	7.2	1.7	2.6	2.6	6.6	3.3
AML6	MDS	Monosomy 7, 11q23 abnormalities	10.5	1.5	18.7	2.3	8.5	2.2	14.7	1.9
AML7	M1	Normal	5.3	1.8	9.9	2.0	3.1	0.2	1.6	1.0
AML8	M2	Normal	7.5	0.8	13.2	2.8	5.1	2.0	8.9	1.4
AML9	MDS	16q22 (cbFBx2)	7.1	2.0	29.7	4.8	1.2	0.3	8.2	0.6
AML10	M5	ND	68.1	12.2	90.7	11.1	7.3	1.2	31.7	2.5
AML11	M2/M4	t(8;21)	3.7	1.4	24.6	2.4	1.7	0.7	14.3	5.8
AML12	M5	Normal	18.5	1.9	37.5	2.7	4.8	1.2	3.3	1.5
AML13	M4	Deletion of chromosome 7	57.3	6.1	53.9	6.3	6.8	1.0	11.2	2.5
AML14	M4	ND	16.9	3.2	25.7	3.3	17.7	2.0	25.0	1.7
Geometric mean	NA	NA	9.3†		24.9		4.9‡		13.8	
95% CI	NA	NA	5.3, 16.2		17.6, 35.1		3.3, 7.5		9.5, 20.1	
CML specimens										
CML1	bcCML	t(9;22)	37.0	0.9	39.3	1.1	8.1	0.5	22.0	1.6
CML2	bcCML	t(9;22)	16.8	2.2	30.8	5.2	16.9	2.2	30.7	7.1
CML3	bcCML	t(9;22)	61.4	0.8	47.0	1.3	19.7	9.4	24.2	6.8
CML4	bcCML	t(9;22)	5.1	2.9	15.6	7.5	5.3	1.0	14.2	3.5
Geometric mean	NA	NA	20.2§		29.9		10.7		21.6	
95% CI	NA	NA	7.5, 54.4		19.1, 47.0		6.4, 18.0		16.4, 28.5	
Normal specimens										
N1	NA	NA	98.4	1.5	93.5	8.1	98.8	1.7	97.5	3.0
N2	NA	NA	85.3	5.5	100.0	0.1	55.0	11.9	100.0	0.3
N3	NA	NA	93.9	18.6	98.5	5.2	71.1	27.1	97.0	8.9
N4	NA	NA	70.6	7.9	84.6	5.0	57.0	16.8	75.0	6.1
N5	NA	NA	92.2	1.8	96.4	2.1	73.5	1.7	95.6	2.3
N6	NA	NA	99.7	1.1	100.0	2.2	96.8	1.2	100.6	2.0
N7	NA	NA	98.8	1.1	97.9	3.8	96.8	1.6	98.9	2.1
Geometric mean	NA	NA	93.4		92.8		86.5		82.1	
95% CI	NA	NA	85.4, 102.2		88.5, 97.2		74.0, 101.2		69.4, 97.1	

ND indicates not determined; and NA, not applicable.

\*Viability normalized to untreated controls.

†10.1-fold lower viability ( $P < .001$ ) than healthy subjects.‡17.5-fold lower viability ( $P < .001$ ) than healthy subjects.§4.6-fold lower viability ( $P = .003$ ) than healthy subjects.||8.1-fold lower viability ( $P < .001$ ) than healthy subjects.

determined by annexin labeling after 18 hours of culture. At a 5- $\mu$ M concentration, most of the AML specimens demonstrated very low viability after 18 hours in culture (mean, 9.3% viable CD34<sup>+</sup> cells; 95% confidence interval [CI], 5.3, 16.2), with the exception of specimens 10 and 13 (68% and 57% viability, respectively). However, the viability of these 2 specimens was greatly reduced by increasing PTL to a concentration of 7.5  $\mu$ M (7.3% and 6.8%, respectively). Overall, the viability of AML CD34<sup>+</sup> cells was more than 10-fold less than normal CD34<sup>+</sup> controls ( $P < .001$ ). Similarly, bcCML cells also showed a strong cytotoxic response to PTL in the 5 to 7.5  $\mu$ M concentration range. In contrast, both the total and CD34<sup>+</sup> cells from normal specimens showed almost no decrease in viability when treated with 5  $\mu$ M PTL (mean, 93.4% viable CD34<sup>+</sup> cells; 95% CI, 85.4, 102.2) and a very modest decrease at 7.5  $\mu$ M PTL (mean, 86.5% viable CD34<sup>+</sup> cells; 95% CI, 74.0, 101.2). Thus, PTL is much more toxic to AML cells than normal, even within the CD34<sup>+</sup> population, which is relatively enriched for progenitors. In order to look more specifi-

cally at primitive stem cell populations, the same suspension culture assays were analyzed with respect to cells bearing a CD34<sup>+</sup>/CD38<sup>-</sup> immunophenotype, which has previously been shown to be characteristic of both normal and AML stem cells.<sup>1</sup> PTL was tested at 0 to 10  $\mu$ M concentrations on all the AML and normal specimens described in Table 1. A representative graph (Figure 1A) using 5 AML specimens demonstrates that the CD34<sup>+</sup>CD38<sup>-</sup> leukemic population is very sensitive to PTL treatment and shows a strong apoptotic response in the 5 to 7.5  $\mu$ M range. Control experiments with normal CD34<sup>+</sup>CD38<sup>-</sup> cells (Figure 1B) show no appreciable toxicity at 5  $\mu$ M PTL and only begin to demonstrate modest effects at 10  $\mu$ M PTL. Thus, phenotypically primitive cells also demonstrate strong AML-specific toxicity in response to PTL.

As a means to further assess the relative efficacy of PTL, we also performed side-by-side comparison studies with the standard chemotherapy drug Ara-C. Analysis of CD34<sup>+</sup>/CD38<sup>-</sup> cells showed Ara-C was more toxic than PTL for normal cells (Figure 1D) while

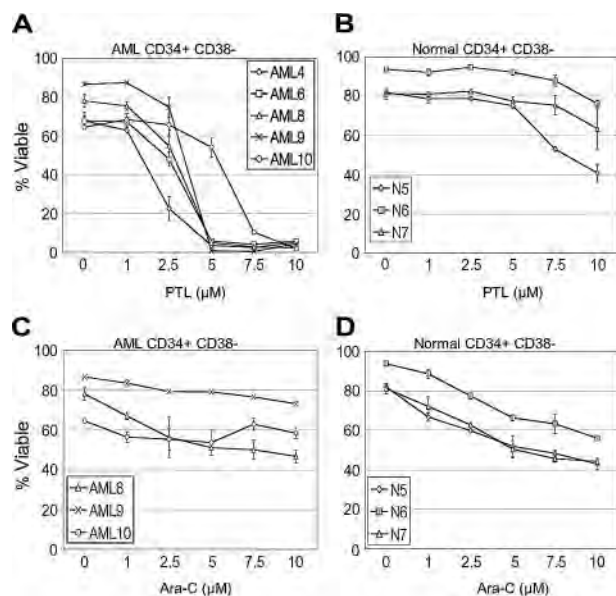


**Figure 1.** PTL induces apoptosis in CD34<sup>+</sup>CD38<sup>-</sup> AML cells but not in normal cells in a dose-dependent manner. In vitro cultures were maintained for 18 hours followed by analysis of viability using annexin-V labeling. Each plot shows the average percent cell viability for CD34<sup>+</sup>CD38<sup>-</sup> AML (A,C) and normal (N) cells (B,D) treated with increasing concentrations of PTL (A-B) or Ara-C (C-D). Each error bar represents the SD. All assays were performed in triplicate.

demonstrating very little toxicity to AML CD34<sup>+</sup>/CD38<sup>-</sup> cells (Figure 1C). This observation is consistent with our previous report that showed reduced Ara-C toxicity to AML CD34<sup>+</sup>/CD38<sup>-</sup> cells in comparison to the overall AML cell population.<sup>8</sup> Furthermore, Ara-C effects on LSC viability appear to plateau at levels above 7.5 μM, even at concentrations as high as 200 μM (data not shown). These experiments indicate that PTL has greater toxicity to AML cells than Ara-C and has less nonspecific toxicity to normal cells.

#### PTL treatment affects leukemic but not normal progenitor and stem cell activity

To functionally assess the effects of PTL treatment, in vitro colony assays and the NOD/SCID mouse xenotransplant model were used to determine whether PTL affected the potential of primitive cells. Different AML and normal specimens were first treated with 5.0 or 7.5 μM PTL for 18 hours followed by analysis using methylcellulose colony assays. Figure 2A shows that AML colony-forming units (CFUs) were dramatically reduced by PTL treatment. In contrast, normal CFUs show little to no effect (Figure 2B) and in some cases are even slightly increased by PTL treatment. Further, from a qualitative perspective, neither the size/morphology of normal colonies nor the frequency of myeloid and erythroid colonies was affected by PTL treatment. The CFU assays demonstrate that preferential targeting of AML cells by PTL is also evident at the progenitor cell level. For comparison, we also treated AML and normal specimens with 5.0 Ara-C μM for 18 hours and then analyzed CFU potential. As shown in Figure 2C, AML CFUs were only reduced by approximately 50%, however; both myeloid and erythroid colonies from normal donors were strongly reduced as a consequence of Ara-C treatment (average ~85% inhibition).

To further validate ablation of primitive cells, the NOD/SCID xenogeneic model was used to assess LSC and HSC potential after PTL treatment. Primary cells were treated with 7.5 μM PTL for 18 hours and then transplanted into sublethally irradiated mice. After 6 to 8 weeks, BM cells were harvested and labeled with antihuman

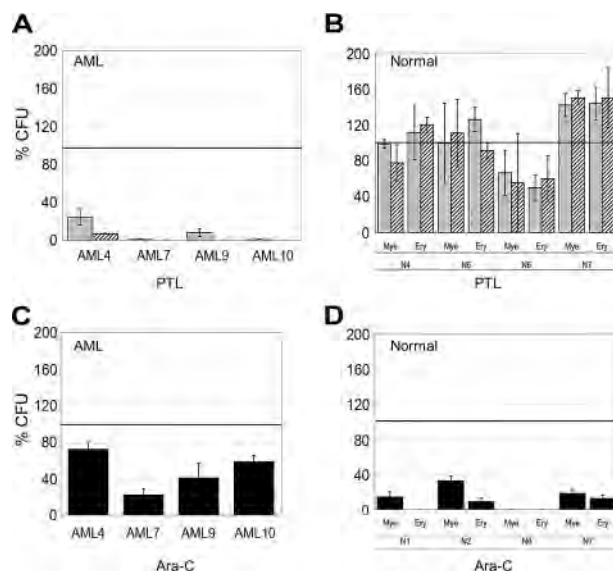


**Figure 2.** In vitro colony assays for AML and normal cells treated with PTL and Ara-C. AML versus normal cells in panels A and B were treated with 5 μM (□) or 7.5 μM PTL (▨). AML versus normal cells in panels C and D were treated with 5 μM Ara-C (■). All treatments were performed for 18 hours in suspension culture, followed by plating in methylcellulose culture. Error bars represent the SD. Average percent of colony-forming units (CFU) are normalized to untreated control (horizontal bar). All assays were performed in triplicate. Mye represents myeloid; Ery, erythroid.

CD45 antibody to determine the percentage of human cells engrafted in each animal. As shown in Figure 3, PTL treatment strongly reduces the ability of LSCs to engraft in the NOD/SCID mouse but did not affect the activity of normal HSCs. In addition, lineage analysis of mice that received a transplant of normal cells show that PTL does not effect in vivo differentiation of myeloid or lymphoid lineages (data not shown). Taken together, these results indicate that PTL is able to induce LSC-specific apoptosis while sparing normal stem and progenitor cells.

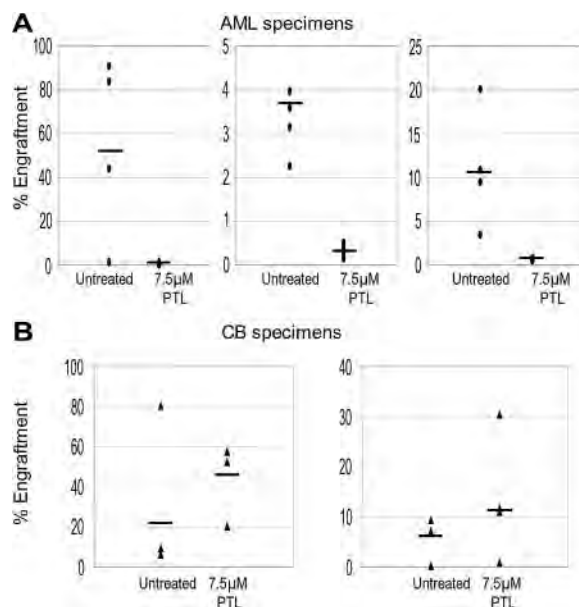


**Figure 3.** PTL inhibits NOD/SCID repopulating ability for AML but not normal cells. Percentage of engraftment for NOD/SCID mice that received a transplant with AML (A) or normal CB (B) cells after 18 hours of culture with or without 7.5 μM PTL. Each ● or ▲ represents a single animal analyzed at 6 to 8 weeks after transplantation. Each plot represents an AML/CB specimen. Mean engraftment is indicated by the horizontal bars.

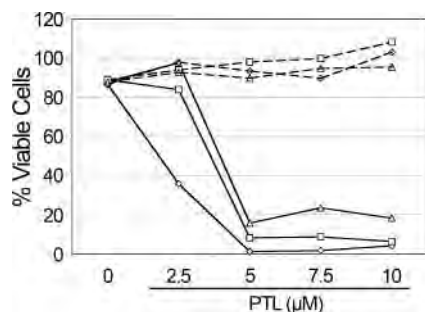


**Figure 4. NAC treatment abolishes PTL apoptosis induction in AML cells.** Percent viability of CD34<sup>+</sup> cells from 3 different AML specimens treated with increasing concentrations of PTL. Cells were precultured with 800  $\mu$ M NAC (---) versus untreated controls (—) for 1 hour and immediately washed and treated with PTL for 18 hours. Specimens shown correspond to AML5 (□), AML10 (◇) and AML15 (△).

#### Parthenolide effects on cell survival are mediated by changes in oxidative state

PTL has been reported to increase intracellular reactive oxygen species (ROS).<sup>11,23</sup> Therefore, to determine whether the rapid apoptosis induced by PTL in AML cells involved redox changes, we precultured cells for 1 hour in 800  $\mu$ M NAC (*N*-acetyl-L-cysteine), a potent antioxidant. Cells were then washed and cultured with different concentrations of PTL. Pretreatment of AML cells with NAC completely abolished the effects of PTL, even at 10- $\mu$ M concentration of drug (Figure 4). These data suggest that an increased oxidative state may be a component of the leukemia cell death mechanism. To further address this possibility, we stained primary AML cells, in the presence or absence of PTL, with DCF (2,7-dichlorodihydrofluorescein diacetate; H<sub>2</sub>DCF-DA), a commonly used redox-sensitive dye. PTL-treated cells showed an increase in DCF fluorescence when compared with untreated cells, consistent with a more oxidized state (data not shown). To test whether increasing ROS alone was sufficient to induce AML apoptosis, we also treated AML cells with buthionine sulfoximine (BSO; data not shown). This treatment had no effect on AML viability. Since the data suggested an increase in ROS as part of the leukemia-specific apoptosis mechanism, we hypothesized that agents that increase ROS might enhance the activity of PTL. This theory was investigated by combining PTL with PGJ2, a natural ligand of peroxisome proliferator-activated receptor- $\gamma$  (PPAR- $\gamma$ ) that has been reported to induce apoptosis of cancer cells by generation of ROS.<sup>29-32</sup> As illustrated in Figure 5, 2.5  $\mu$ M PTL and 0.5  $\mu$ M PGJ2 alone have little to no effect on CD34<sup>+</sup>CD38<sup>-</sup> AML or bcCML cells after 18 hours of treatment. However, when

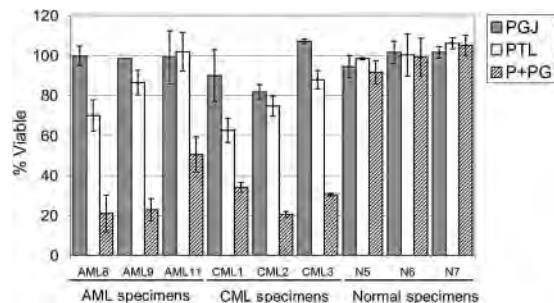


**Figure 5. PGJ2 increases the sensitivity of leukemia cells to PTL.** Average percent viability for CD34<sup>+</sup>CD38<sup>-</sup> cells normalized to untreated controls. Three AML, 3 bcCML, and 3 normal specimens were treated for 18 hours with 0.5  $\mu$ M PGJ2 (□), 2.5  $\mu$ M PTL (□), or both (▨). Each error bar represents the SD. All assays were performed in triplicate.

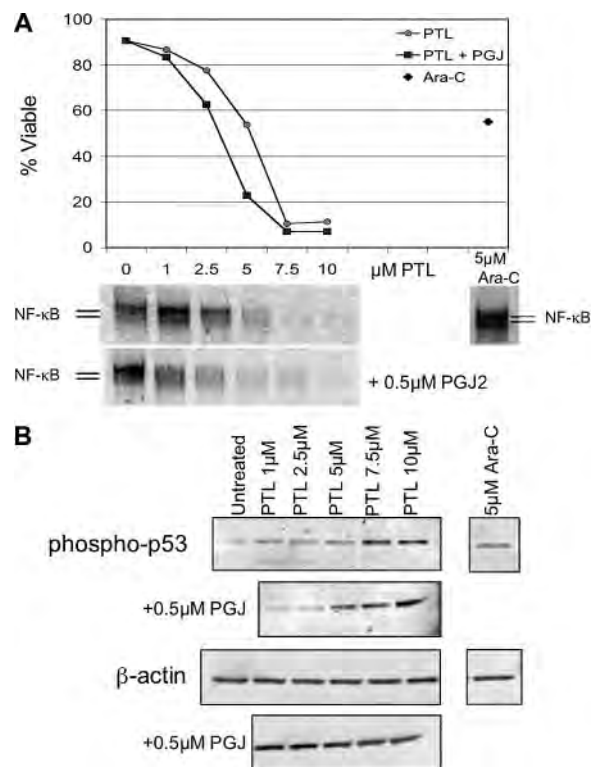


**Figure 6. Apoptosis induction by PTL or PTL/PGJ2 correlates to inhibition of NF- $\kappa$ B and increased phosphorylation of p53(ser15).** (A) Percent viability and NF- $\kappa$ B electrophoretic mobility shift assay (EMSA) of a representative AML specimen treated with increasing concentrations of PTL alone (●) or in combination with 0.5  $\mu$ M PGJ2 (■). The viability is compared with and Ara-C (5  $\mu$ M; ◆) treatments. (B) Immunoblot analysis of phospho-p53(ser15) and actin for the same representative AML specimen treated with increasing dose of PTL 0.5  $\mu$ M PGJ2.

2.5  $\mu$ M PTL is combined with 0.5  $\mu$ M PGJ2, a substantial decrease is observed for both AML and bcCML cells. Moreover, normal CD34<sup>+</sup>CD38<sup>-</sup> hematopoietic cells were not affected by the same treatment. These data suggest a role for redox changes in leukemia-specific apoptosis induction and indicate that PGJ2 can act to sensitize myeloid leukemia cells to PTL.

#### NF- $\kappa$ B inhibition and p53 activation are associated with the AML-specific apoptosis mechanism

NF- $\kappa$ B is constitutively active in AML cells but not in normal hematopoietic cells and its inhibition is correlated with leukemia-specific cell death.<sup>8</sup> In addition, we have reported that p53 is activated when AML cells are treated with the proteasome inhibitor MG-132 in combination with idarubicin.<sup>11</sup> Therefore, we sought to investigate whether common underlying pathways are invoked when leukemia-specific cell death is induced by PTL. To address how NF- $\kappa$ B inhibition correlates with cell death upon PTL or PTL + PGJ2 treatment, DNA-binding assays were performed after 6 hours of treatment. Figure 6A, shows a representative example of EMSA data from 5 independent experiments. The AML viability curve (Figure 6A top panel) illustrates the PTL and PTL + PGJ2 dose response and is compared with the degree of NF- $\kappa$ B inhibition for each concentration of PTL (Figure 6A bottom panel). For comparison, the figure also shows the level of NF- $\kappa$ B activity for Ara-C (5  $\mu$ M) treatment. Clearly, as the inhibition of NF- $\kappa$ B is increased, the survival of the malignant cells is decreased. Moreover, in the case of PTL + PGJ2 treatment, the cells are more sensitive and displayed a lower NF- $\kappa$ B activity when compared

with the same concentration of PTL alone. In contrast, treatment with 5  $\mu$ M Ara-C showed an increase in NF- $\kappa$ B activity, as has been reported for many chemotherapeutic drugs. This suggests that there exists a direct correlation between NF- $\kappa$ B inhibition and the sensitivity of the AML cells to undergo apoptosis. To determine the degree of proapoptotic p53 activation, immunoblots were performed using phospho-ser15-specific anti-p53 antibody. Figure 6B (top panel) shows an increase in p53-ser15 phosphorylation upon PTL and PTL + PGJ2 treatments. As cell death is increased, p53-ser15 phosphorylation increases as well. In addition, PTL in combination with PGJ2 shows even higher levels of phospho-p53-ser15. In the case of Ara-C treatment, we observed some increase in p53-ser15 phosphorylation; however, in the absence of NF- $\kappa$ B inhibition, we propose that any p53-mediated proapoptotic activity is abrogated by NF- $\kappa$ B-mediated survival signals.

## Discussion

These studies demonstrate that PTL is able to induce rapid and robust death of myeloid leukemia cells. Our experiments show that an 18-hour treatment with PTL at 5 to 7.5  $\mu$ M is highly toxic to total AML and bcCML populations, phenotypically primitive (CD34<sup>+</sup>/CD38<sup>-</sup>) AML cells, AML colony-forming cells, and AML stem cells as assayed by engraftment of NOD/SCID mice. In contrast, normal hematopoietic cells were almost completely unaffected by the same conditions. Thus, not only is PTL a potent antileukemia agent, it has no significant toxicity to normal cells at the concentrations tested. By comparison, analysis of the commonly used leukemia drug Ara-C showed modest toxicity to AML cells and relatively high toxicity to normal cells. Increased concentrations of Ara-C can be achieved in clinical studies (~50-100  $\mu$ M), which may result in greater AML cell killing; however, we did not generally test higher levels because of the strong cytotoxicity observed for normal cells at 5 to 10  $\mu$ M. Taken together, these data suggest that PTL has intriguing potential as an antileukemia agent, particularly with regard to primitive AML stem and progenitor cells. These data also indicate that PTL may be useful for bcCML, but due to limited specimen availability we have only performed the preliminary studies shown in Table 1 and Figure 5.

Previous studies have described several characteristics of PTL in other cell systems. Perhaps most importantly, PTL is known to be a potent inhibitor of NF- $\kappa$ B.<sup>33</sup> The mechanism of NF- $\kappa$ B down-regulation appears to occur via inhibition of the IKK complex. We also observed strong inhibition of NF- $\kappa$ B in primary AML cells and speculate that this activity contributes to the efficacy of PTL. However, our previous genetic studies using a dominant-negative repressor of NF- $\kappa$ B activity have shown that inhibition of NF- $\kappa$ B alone is not sufficient to mediate the robust cell death observed with PTL. Rather, blockade of the NF- $\kappa$ B pathway appears to sensitize primary AML cells to death and induces a relatively slow spontaneous apoptosis (~50% cell death in 36 hours).<sup>11</sup> Similarly, studies by Romano et al<sup>34</sup> showed that treatment of primary AML blasts with NF- $\kappa$ B decoy oligonucleotides was not sufficient to induce a strong apoptotic response. Consequently, PTL must be affecting other pathways relevant to AML-specific survival. One such pathway appears to be mediated by the activity of p53. PTL induced rapid up-regulation of p53 protein with concomitant phosphorylation on serine 15. We have previously shown that activation of this pathway in AML cells

up-regulates p53 proapoptotic target genes such as Bcl-2 associated X protein (Bax), p21, and growth arrest and DNA damage inducible protein (GADD45). Thus, we speculate that p53 activation is one component of the AML-specific cell death mechanism.

Another activity described for PTL is the induction of ROS. Indeed, antitumor activity of PTL has been strongly linked to the increased oxidative state observed during PTL treatment of other tumor types (eg, colorectal and hepatic cancers).<sup>13,27</sup> We observed that pretreatment of AML cells with the free radical scavenger *N*-acetylcysteine completely abrogated PTL-mediated cell death. Notably, the NF- $\kappa$ B inhibitory activity of PTL was also completely blocked by NAC (data not shown). These data indicate that primitive AML cells may be more sensitive to changes in oxidative state than normal cells and that increased ROS contributes to AML-specific cell death. Interestingly, many chemotherapeutic agents are known to increase ROS, but such agents also typically up-regulate NF- $\kappa$ B activity. Our data indicate that inhibition of NF- $\kappa$ B may sensitize AML cells to simultaneous increases in ROS. If true, then one interesting future use of PTL may be a chemosensitizing agent in combination with several common antileukemia drugs. Indeed, a recent study by Nakshatri et al<sup>18</sup> showed that PTL reverses resistance of cancer cells to TRAIL (tumor necrosis factor [TNF]-related apoptosis-inducing ligand). Previous reports with other drugs such as bortezomib also suggest NF- $\kappa$ B inhibition can be used to augment the response of cancer cells to chemotherapy agents.<sup>35,36</sup>

The naturally occurring prostaglandin PGJ2 has antiproliferative and proapoptotic effects in different types of cancer cells.<sup>29-32,37,38</sup> PGJ2 is an inhibitor of NF- $\kappa$ B activation<sup>39</sup> and can also induce intracellular oxidative stress.<sup>40</sup> When low concentrations (0.5  $\mu$ M) of PGJ2 were combined with low concentrations of PTL (2.5  $\mu$ M), a cooperative effect was observed with respect to both cell death and modulation of NF- $\kappa$ B and p53. Thus, PGJ2 appears to enhance the activity of PTL and/or affect other pathways relevant to leukemia cell survival.

Taken together, the results of the present study confirm and extend data for a model we have previously described to explain unique aspects of LSC survival.<sup>41</sup> From a general perspective, when AML stem and progenitor cells are deprived of survival signals and simultaneously exposed to cellular stress, they appear to be preferentially sensitized to cell death. We propose that inhibition of NF- $\kappa$ B, proapoptotic activation of p53, and increased oxidative stress are among the molecular changes that occur to mediate this event. Importantly, these specific events were noted in the present studies with PTL and in earlier studies using MG-132 and idarubicin. Thus, 2 completely disparate chemical approaches to LSC-specific apoptosis display these common molecular changes. Further, we observed that while Ara-C treatment produced p53 (ser-15) phosphorylation at levels similar to PTL, NF- $\kappa$ B was not inhibited. Therefore, the cellular response to Ara-C does not meet the criteria observed for PTL-induced LSC apoptosis.

Although PTL very effectively induces LSC-specific cell death and appears to be a good candidate for AML therapy, its pharmacologic properties may be limiting. In a dose escalation study for Feverfew, PTL plasma levels were well below the concentrations that showed an effect on AML survival.<sup>42</sup> In vitro studies using purified material indicate PTL is only soluble to approximately 1.0 mg/mL in aqueous solutions and therefore may be difficult to deliver at concentrations sufficient for leukemia therapy. However, recent studies have shown that the PTL molecule can be chemically modified to improve water solubility by 100- to 1000-fold (P. Crooks, University of Kentucky, personal written communication,

January 2004). Several such analogs appear to retain their antitumor properties and are currently being tested for in vivo efficacy.

In summary, this study demonstrates that selective targeting of LSCs is possible by exploiting unique molecular characteristics of leukemic cells. PTL as a single agent induces cooperating molecular events that are sufficient to cause LSC-specific cell death in vitro. This biologic activity can be abrogated by changes in redox state or enhanced by the added effects of PGJ2 treatment. Going forward, the main challenge will be to translate these findings to a

clinically relevant setting and demonstrate that LSCs can be targeted in vivo.

## Acknowledgments

We gratefully acknowledge Drs Fay Young and James Palis for critical review of the manuscript.

## References

- Bonnet D, Dick JE. Human acute myeloid leukemia is organized as a hierarchy that originates from a primitive hematopoietic cell. *Nat Med*. 1997;3:730-737.
- Blair A, Hogge DE, Sutherland HJ. Most acute myeloid leukemia progenitor cells with long-term proliferative ability in vitro and in vivo have the phenotype CD34(+)CD71(-)/HLA-DR. *Blood*. 1998;92:4325-4335.
- Lapidot T, Sirard C, Vormoor J, et al. A cell initiating human acute myeloid leukaemia after transplantation into SCID mice. *Nature*. 1994;367:645-648.
- Blair A, Hogge DE, Ailles LE, Lansdorp PM, Sutherland HJ. Lack of expression of Thy-1 (CD90) on acute myeloid leukemia cells with long-term proliferative ability in vitro and in vivo. *Blood*. 1997;89:3104-3112.
- Blair A, Sutherland HJ. Primitive acute myeloid leukemia cells with long-term proliferative ability in vitro and in vivo lack surface expression of c-kit (CD117). *Exp Hematol*. 2000;28:660-671.
- Jordan CT, Upchurch D, Szilvassy SJ, et al. The interleukin-3 receptor alpha chain is a unique marker for human acute myelogenous leukemia stem cells. *Leukemia*. 2000;14:1777-1784.
- Guan Y, Gerhard B, Hogge DE. Detection, isolation, and stimulation of quiescent primitive leukemic progenitor cells from patients with acute myeloid leukemia (AML). *Blood*. 2003;101:3142-3149.
- Guzman ML, Neering SJ, Upchurch D, et al. Nuclear factor-kappaB is constitutively activated in primitive human acute myelogenous leukemia cells. *Blood*. 2001;98:2301-2307.
- Hope KJ, Jin L, Dick JE. Acute myeloid leukemia originates from a hierarchy of leukemic stem cell classes that differ in self-renewal capacity. *Nat Immunol*. 2004;5:738-743.
- Guzman ML, Upchurch D, Grimes B, et al. Expression of tumor-suppressor genes interferon regulatory factor 1 and death-associated protein kinase in primitive acute myelogenous leukemia cells. *Blood*. 2001;97:2177-2179.
- Guzman ML, Swiderski CF, Howard DS, et al. Preferential induction of apoptosis for primary human leukemic stem cells. *Proc Natl Acad Sci U S A*. 2002;99:16220-16225.
- Knight DW. Feverfew: chemistry and biological activity. *Nat Prod Rep*. 1995;12:271-276.
- Zhang S, Ong CN, Shen HM. Critical roles of intracellular thiols and calcium in parthenolide-induced apoptosis in human colorectal cancer cells. *Cancer Lett*. 2004;208:143-153.
- Ross JJ, Arnason JT, Birnboim HC. Low concentrations of the feverfew component parthenolide inhibit in vitro growth of tumor lines in a cytostatic fashion. *Planta Med*. 1999;65:126-129.
- Wojnarowski JM, Konopa J. Inhibition of DNA biosynthesis in HeLa cells by cytotoxic and antitumor sesquiterpene lactones. *Mol Pharmacol*. 1981;19:97-102.
- Wiedhopf RM, Young M, Bianchi E, Cole JR. Tumor inhibitory agent from *Magnolia grandiflora* (Magnoliaceae), I: parthenolide. *J Pharm Sci*. 1973;62:345.
- Zhang S, Lin ZN, Yang CF, Shi X, Ong CN, Shen HM. Suppressed NF-(kappa)B and sustained JNK activation contribute to the sensitization effect of parthenolide to TNF-(alpha)-induced apoptosis in human cancer cells. *Carcinogenesis*. 2004;25:2191-2199.
- Nakshatri H, Rice SE, Bhat-Nakshatri P. Antitumor agent parthenolide reverses resistance of breast cancer cells to tumor necrosis factor-related apoptosis-inducing ligand through sustained activation of c-Jun N-terminal kinase. *Oncogene*. 2004;23:7330-7344.
- deGraffenried LA, Chandrasekar B, Friedrichs WE, et al. NF-kappa B inhibition markedly enhances sensitivity of resistant breast cancer tumor cells to tamoxifen. *Ann Oncol*. 2004;15:885-890.
- Patel NM, Nozaki S, Shortle NH, et al. Paclitaxel sensitivity of breast cancer cells with constitutively active NF-kappaB is enhanced by IkappaBalpha super-repressor and parthenolide. *Oncogene*. 2000;19:4159-4169.
- Won YK, Ong CN, Shi X, Shen HM. Chemopreventive activity of parthenolide against UVB-induced skin cancer and its mechanisms. *Carcinogenesis*. 2004;25:1449-1458.
- Kwok BH, Koh B, Nduhuisi MI, Eloffson M, Crews CM. The anti-inflammatory natural product parthenolide from the medicinal herb Feverfew directly binds to and inhibits IkappaB kinase. *Chem Biol*. 2001;8:759-766.
- Hehner SP, Hofmann TG, Droge W, Schmitz ML. The antiinflammatory sesquiterpene lactone parthenolide inhibits NF-kappa B by targeting the I kappa B kinase complex. *J Immunol*. 1999;163:5617-5623.
- Garcia-Pineros AJ, Lindenmeyer MT, Merfort I. Role of cysteine residues of p65/NF-kappaB on the inhibition by the sesquiterpene lactone parthenolide and N-ethyl maleimide, and on its transactivating potential. *Life Sci*. 2004;75:841-856.
- Garcia-Pineros AJ, Castro V, Mora G, et al. Cysteine 38 in p65/NF-kappaB plays a crucial role in DNA binding inhibition by sesquiterpene lactones. *J Biol Chem*. 2001;276:39713-39720.
- Sobota R, Szwed M, Kasza A, Bugno M, Kordula T. Parthenolide inhibits activation of signal transducers and activators of transcription (STATs) induced by cytokines of the IL-6 family. *Biochem Biophys Res Commun*. 2000;267:329-333.
- Wen J, You KR, Lee SY, Song CH, Kim DG. Oxidative stress-mediated apoptosis: the anticancer effect of the sesquiterpene lactone parthenolide. *J Biol Chem*. 2002;277:38954-38964.
- Lansdorp PM, Dragowska W. Long-term erythropoiesis from constant numbers of CD34+ cells in serum-free cultures initiated with highly purified progenitor cells from human bone marrow. *J Exp Med*. 1992;175:1501-1509.
- Okano H, Shiraki K, Inoue H, et al. 15-deoxy-delta-12-14-PGJ2 regulates apoptosis induction and nuclear factor-kappaB activation via a peroxisome proliferator-activated receptor-gamma-independent mechanism in hepatocellular carcinoma. *Lab Invest*. 2003;83:1529-1539.
- Kim BE, Roh SR, Kim JW, Jeong SW, Kim IK. Cytochrome C-dependent Fas-independent apoptotic pathway in HeLa cells induced by delta12-prostaglandin J2. *Exp Mol Med*. 2003;35:290-300.
- Eibl G, Wente MN, Reber HA, Hines OJ. Peroxisome proliferator-activated receptor gamma induces pancreatic cancer cell apoptosis. *Biochem Biophys Res Commun*. 2001;287:522-529.
- Kondo M, Shibata T, Kumagai T, et al. 15-Deoxy-Delta(12,14)-prostaglandin J(2): the endogenous electrophile that induces neuronal apoptosis. *Proc Natl Acad Sci U S A*. 2002;99:7367-7372.
- Bork PM, Schmitz ML, Kuhnt M, Escher C, Heinrich M. Sesquiterpene lactone containing Mexican Indian medicinal plants and pure sesquiterpene lactones as potent inhibitors of transcription factor NF-kappaB. *FEBS Lett*. 1997;402:85-90.
- Romano MF, Lamberti A, Bisogni R, et al. Enhancement of cytosine arabinoside-induced apoptosis in human myeloblastic leukemia cells by NF-kappa B/Rel- specific decoy oligodeoxynucleotides. *Gene Ther*. 2000;7:1234-1237.
- Amiri KI, Horton LW, LaFleur BJ, Sosman JA, Richmond A. Augmenting chemosensitivity of malignant melanoma tumors via proteasome inhibition: implication for bortezomib (VELCADE, PS-341) as a therapeutic agent for malignant melanoma. *Cancer Res*. 2004;64:4912-4918.
- An J, Sun Y, Fisher M, Rettig MB. Antitumor effects of bortezomib (PS-341) on primary effusion lymphomas. *Leukemia*. 2004;18:1699-1704.
- Fukuchi K, Date M, Azuma Y, Shinohara M, Takahashi H, Ohura K. Apoptosis in human oral squamous cell carcinomas is induced by 15-deoxy-delta 12,14-prostaglandin J2 but not by troglitazone. *J Dent Res*. 2003;82:802-806.
- Clay CE, Monjazeab A, Thorburn J, Chilton FH, High KP. 15-Deoxy-delta12,14-prostaglandin J2-induced apoptosis does not require PPARgamma in breast cancer cells. *J Lipid Res*. 2002;43:1818-1828.
- Straus DS, Pascual G, Li M, et al. 15-deoxy-delta 12,14-prostaglandin J2 inhibits multiple steps in the NF-kappa B signaling pathway. *Proc Natl Acad Sci U S A*. 2000;97:4844-4849.
- Kondo M, Oya-Ito T, Kumagai T, Osawa T, Uchida K. Cyclopentenone prostaglandins as potential inducers of intracellular oxidative stress. *J Biol Chem*. 2001;276:12076-12083.
- Guzman ML, Jordan CT. Considerations for targeting malignant stem cells in leukemia. *Cancer Control*. 2004;11:97-104.
- Curry EA 3rd, Murry DJ, Yoder C, et al. Phase I dose escalation trial of feverfew with standardized doses of parthenolide in patients with cancer. *Invest New Drugs*. 2004;22:299-305.

## APPENDIX #2

### **An orally bioavailable parthenolide analog selectively eradicates acute myelogenous leukemia stem and progenitor cells**

**Running Title:** A parthenolide analog targets leukemia stem cells

Monica L. Guzman<sup>1</sup>, Randall M. Rossi<sup>1</sup>, Sundar Neelakantan<sup>2</sup>, Xiaojie Li<sup>1</sup>, Cheryl Corbett<sup>1</sup>, Duane C. Hassane<sup>1</sup>, Michael W. Becker<sup>1</sup>, John M. Bennett<sup>1</sup>, Edmund Sullivan<sup>3</sup>, Joshua L. Lachowicz<sup>4</sup>, Christopher J. Sweeney<sup>5</sup>, William Matthews<sup>6</sup>, Martin Carroll<sup>7</sup>, Jane L. Liesveld<sup>1</sup>, Peter A. Crooks<sup>2</sup>, and Craig T. Jordan<sup>1</sup>.

<sup>1</sup> James P. Wilmot Cancer Center, University of Rochester, Rochester, NY, 14642.

<sup>2</sup> College of Pharmacy, University of Kentucky, Lexington, KY, United States, 40536.

<sup>3</sup> Advanced Veterinary Services, Bellingham, WA.

<sup>4</sup> Redbank Veterinary Hospital, Tinton Falls, NJ, 07724.

<sup>5</sup> Department of Medicine, Indiana University School of Medicine, Indianapolis, United States, 46202.

<sup>6</sup> Leuchemix Inc., Woodside, CA, United States, 94062.

<sup>7</sup> Division of Hematology and Oncology, University of Pennsylvania, Philadelphia, PA, United States, 19104.

#### **Corresponding Author:**

Craig T. Jordan, PhD  
University of Rochester Medical Center  
601 Elmwood Ave. Box 703  
Rochester, NY, 14642, United States  
Telephone: 585-275-6339  
Email: craig\_jordan@urmc.rochester.edu

**Text word count:** 4705

**Abstract word count:** 200

**Category:** Neoplasia

## Abstract

Leukemia stem cells (LSCs) are thought to play a central role in the pathogenesis of acute leukemia and likely contribute to both disease initiation and relapse. Therefore, identification of agents that target LSCs is an important consideration for the development of new therapies. To this end, we have previously demonstrated that the naturally-occurring compound parthenolide (PTL) can induce death of human LSCs *in vitro*, while sparing normal hematopoietic cells. However, PTL has relatively poor pharmacological properties that limit its potential clinical use. Consequently, we generated a family of PTL analogs designed to improve solubility and bioavailability. These studies identified an analog, dimethylamino-parthenolide (DMAPT), which induces rapid death of primary human LSC from both myeloid and lymphoid leukemias, and is also highly cytotoxic to bulk leukemic cell populations. Molecular studies indicate the prevalent activities of DMAPT include induction of oxidative stress responses, inhibition of NF- $\kappa$ B, and activation of p53. The compound has approximately 70% oral bioavailability and pharmacological studies using both mouse xenograft models and spontaneous acute canine leukemias demonstrate *in vivo* bioactivity as determined by multiple biomarkers. Therefore, based on the collective preclinical data, we propose that the novel compound DMAPT has the potential to target human LSCs *in vivo*.

## Introduction

Recent studies have demonstrated that myeloid and certain forms of lymphoid leukemia arise from malignant stem cells (termed leukemia stem cells, LSCs).<sup>1-3</sup> Unlike the bulk leukemia population, LSCs are found in a quiescent state and are thus unlikely to respond to standard chemotherapeutic agents which preferentially eradicate actively cycling cells.<sup>4-7</sup> Indeed, the persistence of LSCs following chemotherapy may be a major factor contributing to clinical relapse.<sup>8,9</sup> In addition, conventional leukemia therapy is also substantially toxic to normal hematopoietic cells and frequently results in severe myelosuppression. Therefore, given the drug refractory nature of LSCs, and the importance of normal hematopoiesis, identification of less toxic and more specific forms of therapy are important priorities for the development of better therapeutic regimens.

As a foundation for developing more selective leukemia treatments, our previous studies have investigated basic properties of primitive AML cells. These studies showed that LSCs from different AML subtypes share characteristics<sup>10</sup> which are unique to AML and thus represent potential therapeutic targets for the selective ablation of LSCs relative to their normal counterparts.<sup>11,12</sup> Specifically, we reported that NF- $\kappa$ B, a known regulator of growth and survival, is constitutively active in LSCs but not in HSCs.<sup>13</sup> Notably, many traditional cancer therapies induce activation of NF- $\kappa$ B, a potentially undesirable characteristic likely to facilitate survival of malignant cells.<sup>14,15</sup> Given the ability of many cancer cells to evade apoptosis, we hypothesized that NF- $\kappa$ B inhibition could be used to facilitate LSC-selective cell death, a concept supported by studies using the proteasome inhibitor MG-132 (known to inhibit NF- $\kappa$ B) with the anthracycline Idarubicin (IDR).<sup>16</sup> However, molecular genetic approaches demonstrated that NF- $\kappa$ B inhibition alone is not sufficient to strongly induce AML-specific apoptosis. Further investigation of pathways induced by MG-132 + IDR treatment revealed activation of p53 and increased oxidative load as prevalent components of the AML cell death process.<sup>7</sup> Collectively, these data suggest that the mechanism of LSC death involves combined inhibition of survival pathways and activation of tumor suppressor and/or stress pathways.<sup>17</sup> More recently, we have shown that robust apoptosis of

primary AML cells can be achieved with a single agent, the plant derived compound parthenolide (PTL), an agent known to induce oxidative stress and inhibit NF- $\kappa$ B.<sup>7</sup> Importantly, PTL also effectively eradicates AML stem and progenitor cells *in vitro* while sparing normal hematopoietic cells. Hence, PTL has the ability to eradicate AML stem cells, as well as to ablate bulk leukemia blast cells; properties that should make this compound an attractive agent for clinical evaluation. However, despite the utility of PTL determined by *in vitro* studies, its solubility is relatively poor, making pharmacological use of the compound difficult. In animal studies, maximum attainable serum levels were 200nM,<sup>18</sup> a concentration approximately 30 fold less than required to mediate LSC cell death *in vitro*. Therefore, we have synthesized and screened PTL analogs to identify a compound with improved solubility and bioavailability. These studies have generated a dimethylamino analog of parthenolide (DMAPT). When formulated as a fumarate salt DMAPT demonstrates over 1000 fold greater solubility in water relative to PTL (Neelakantan et al., manuscript in preparation). Moreover, as shown in the present studies, DMAPT effectively eliminates human AML stem and progenitor cells without apparent harm to normal hematopoietic stem and progenitor cells. The compound also eradicates phenotypically primitive blast crisis CML and acute lymphoblastic leukemia (ALL) cells. The molecular responses to DMAPT, both *in vitro* and *in vivo*, include activation of cellular stress responses and inhibition of NF- $\kappa$ B. Together, the data suggest that DMAPT represents a clinical candidate for leukemia therapy with the potential to target leukemia stem and progenitor cells.

## **Materials and Methods**

### **Cell Isolation and Culture**

Primary human AML, CML, ALL cells, and normal bone marrow (BM) cells were obtained from volunteer donors with informed consent. Umbilical cord blood (CB) was obtained from the National Disease Research Interchange (NDRI). Dog samples were obtained from Bellingham Veterinary Clinic, Colorado State University (Department of Pathology) or Redbank Veterinary Hospital (Case Study II). Mononuclear cells were isolated from the samples using Ficoll-Plaque (Pharmacia Biotech, Piscataway, NY) density gradient separation. For canine case studies WBC numbers were determined using The HESKA<sup>®</sup> CBC-Diff<sup>™</sup> System. In some cases cells were cryopreserved in freezing medium of Iscove's modified Dulbecco medium (IMDM), 40% fetal bovine serum (FBS), and 10% dimethylsulfoxide (DMSO) or in CryoStor<sup>™</sup> CS-10 (VWR). Cells were cultured in serum-free medium (SFM)<sup>19</sup> for 1h before the addition of DMAPT. Parthenolide was obtained from Biomol (Plymouth Meeting, PA).

### **DMAPT synthesis and pharmacology**

DMAPT was prepared from the reaction of parthenolide with dimethylamine, and the result dimethylamino analog was then converted to its water-soluble fumarate salt. The detailed synthesis, structural identity and stereochemistry of DMAPT are reported elsewhere (Neelakantan et al., manuscript in preparation). Bioavailability and pharmacokinetic assays for rodents were performed by the Developmental Therapeutics Program from the National Cancer Institute and for dogs by Integrated Analytical Solutions, Berkeley, CA.

### **Methylcellulose Colony-Forming Assay**

AML, BM or CB cells were cultured in SFM as above for 18h in the presence or absence of DMAPT. Cells were plated at 50,000 cells/ml in Methocult GFH4534 (Stem Cell Technologies, Vancouver) supplemented with Erythropoietin 3U/ml and G-CSF 50ng/ml. Colonies were scored after 10-14 days of culture.

### **Electrophoretic Mobility Shift Assay (EMSA), and Immunoblot Analysis**

EMSA was performed as described.<sup>13</sup> Briefly, nuclear extracts equivalent to 200,000 cells were incubated with 2µg of poly-d(I-C) (Roche Molecular Biochemicals, Indianapolis, IN) and  $10^{-14}$ mol  $^{32}$ P-labeled NF-κB probe in 10mM HEPES, 5mM Tris, 50mM KCl, 1.2mM EDTA and 10% glycerol for 15 minutes at room temperature. Protein/DNA complexes were resolved on a native polyacrylamide gel in 0.25X TBE. For immunoblots, cells were prepared and analyzed as previously described.<sup>11</sup> Blots were probed with anti-phospho-p53 (ser15) from Cell Signaling (Beverly, MA), and anti-actin (AC-15) from Sigma (St. Louis, MO).

### **Confocal microscopy**

Cells were fixed in methanol at -20°C. The cells were permeabilized with blocking buffer (10% FBS and 0.1% Tween 20 in 1x PBS [pH 7.4]) as described.<sup>20</sup> Cells were stained using either rabbit polyclonal anti-p65 (C-20), anti-Nrf-2 (C-20) (Santa Cruz Biotechnologies, Santa Cruz, CA), anti-HO1 (GeneTex Inc., San Antonio, TX) or mouse monoclonal anti-γH2AX (Upstate Biotech, Charlottesville, VA) in blocking buffer for 2 hours at room temperature. Cells were washed and stained with either goat-anti-rabbit Alexa488 or goat-anti-mouse Alexa 488 (Invitrogen, Carlsbad, CA) secondary antibodies and ToPro3 for nuclear stain (Invitrogen). Slides were mounted using Fluoromount-G™ (Southern Biotech, Birmingham, AL). Slides were left to dry overnight. Fluorescence was observed using a 100x objective, further magnified by a 2x zoom, on a Leica inverted scanning confocal microscope.

### **Flow Cytometry**

Apoptosis assays were performed as described.<sup>13</sup> Briefly, after 18-24h of treatment, normal and AML specimens were stained for the surface antibodies CD38-allophycocyanin (APC), CD34-PECy7, CD123-phycoerythrin (Becton Dickinson, San Jose, CA) for 15 minutes. Cells were washed in cold PBS and resuspended in 200µl of annexin-V buffer (0.01M HEPES/NaOH, 0.14M NaCl, 2.5mM CaCl<sub>2</sub>) Annexin-V-fluorescein isothiocyanate (FITC) and 7-aminoactinomycin (7-AAD; Molecular Probes, Eugene, OR) were added and the tubes were incubated at room temperature for 15

minutes then analyzed on a BD LSRII flow cytometer. To analyze human cell engraftment in the NOD/SCID xenotransplant model, BM cells were blocked with the anti-Fc receptor antibody 2.4G2 and 25% human serum and later labeled with anti-human CD45-PE antibody (Becton Dickinson, San Jose, CA). For canine studies cells were stained with CD45-FITC (YKIX716.13; Serotec, Raleigh, NC), CD14-PeCy5 (TUK4; Serotec), CD34-PE (1H6; Becton Dickinson) (Serotec) for 30 minutes. Cells were washed and resuspended in FACS buffer (0.5% FBS in PBS) with 5 µg/ml of DAPI.

### **Non-obese Diabetic (NOD)/Severe Combined Immunodeficient (SCID) Mouse Assays**

NOD/SCID were sub-lethally irradiated with 270 rad using a RadSource-2000 x-ray irradiator before transplantation. Cells to be assayed were injected via tail vein (5-10 million cells) in a final volume of 0.2ml of PBS with 0.5% FBS. After 6-8 weeks, animals were sacrificed, and BM was analyzed for the presence of human cells by flow cytometry.

### **Canine studies**

In vitro and in vivo studies were performed with owner's consent on two animals with a diagnosis of acute leukemia.

Case study I – the subject was an 8 year old male Labrador retriever. At the initiation of treatment the animal was in advanced stages of disease, and received anti-inflammatory agents, sedatives, diuretics, antibiotics, and prokinetic agents as needed during the course of DMAPT treatments. In addition, the dog received 40 mg of prednisone starting at day 5, reduced to 20 mg on day 11 and Mesna 500 mg (3 x day) starting on day 8.

Case study II – the subject was an 8 year old male mixed breed dog. At the beginning of treatment the WBC was highly elevated (81K/ul) and the animal was receiving Deramaxx 100mg SID. At day 15, the animal also began receiving clavamox and prednisone. At day 24 the animal was withdrawn from study at the owner's request due to concern there was not sufficient likelihood of cure to warrant continued treatment.

**U937 differentiation assay**

U937 cells were plated at 400,000 cells/ml and treated with DMAPT (2.5 $\mu$ M or 5 $\mu$ M) or 5 $\mu$ M ATRA. Cells were counted and analyzed 72 hours after treatment for expression of CD 11b and viability (DAPI).

**Statistical analysis**

Statistical analyses and graphs were performed using GraphPad Prism software (GraphPad Software, San Diego, CA). For statistical analysis the data was log transformed and analyzed by one-way ANOVA followed by Tukey post-hoc test. For 2 group comparisons, significance was determined by paired t-tests.

## Results

### **DMAPT selectively eradicates primitive leukemia cells**

DMAPT was prepared from the reaction of PTL with dimethylamine, and the resulting dimethylamino analog was then converted to its water-soluble fumarate salt (Neelakantan et al., manuscript in preparation). Initially, we performed detailed biological studies to determine the efficiency and specificity of anti-leukemia properties for DMAPT. Figure 1A shows that 24-hour exposure of primary human AML cells to either 7.5  $\mu$ M PTL or DMAPT results in similar mean viability in total and CD34+ cell populations (25% vs. 24%, and 12% vs. 12% respectively, n=25 for PTL and n=39 for DMAPT). We further investigated the levels of cell death in phenotypically primitive AML stem cells (CD34+CD38-CD123+). Figure 1B shows the results of cells treated with DMAPT where 5.0 $\mu$ M and 7.5 $\mu$ M concentrations resulted in 15.10% (n=19) and 6.84% (n=21) mean viability respectively. Taken together, the data in Figures 1A and 1B indicate that DMAPT is highly cytotoxic to both overall AML blast cells, as well as the AML stem cell population. To extend our analyses of DMAPT, we also examined other hematological disorders known to derive from malignant stem cells. Figure 1C and 1D show the effect of DMAPT on phenotypically described B-ALL stem/progenitor cells (CD34+CD10-)<sup>3</sup> and CML stem/progenitor cells (CD34+CD38-).<sup>4</sup> These experiments indicate DMAPT also has utility for lymphoid and chronic myeloid forms of leukemia. Finally, to verify the specificity of DMAPT for malignant cells, viability of normal hematopoietic cells was determined. The data in Figure 1E demonstrate that DMAPT does not significantly affect viability of normal CD34+ or CD34+CD38- hematopoietic cells obtained from healthy donors (n=8; p >0.05). Indeed, the mean viability at 5 $\mu$ M DMAPT was 96% for CD34+ cells and 88% for CD34+CD38- cells. At 7.5 $\mu$ M, the mean viability for both CD34+ and CD34+CD38- populations was over 79%. Together, the data demonstrate that DMAPT not only induces rapid cell death in phenotypically described AML, CML and ALL stem/progenitor cells, but is also well tolerated by normal stem and progenitor cells.

## **Functional assays demonstrate that DMAPT ablates primary human AML stem and progenitor cells**

*In vitro* colony assays and NOD/SCID xenotransplant experiments were used to determine whether DMAPT targets functionally defined leukemia progenitor and stem cells. Treatment of normal hematopoietic cells with 5 $\mu$ M DMAPT did not affect myeloid or erythroid colony formation relative to untreated controls (Figure 2A.  $P > 0.05$ ,  $n=5$ ). In contrast, DMAPT treatment strongly inhibited the ability of AML cells to form colonies (mean viability= 6.58%,  $P < 0.001$ ,  $n=10$ ), indicating selective targeting of leukemic progenitor cell populations. Similarly, 18-hour treatment of primary AML cells with DMAPT dramatically inhibited engraftment of sub-lethally irradiated NOD/SCID mice (representative example shown in Figure 2B). Analysis of four independent AML specimens decreased engraftment by 98.2% ( $n=5$  mice,  $p<0.0001$ ), 91% ( $n=5$ ,  $p=0.001$ ), 90% ( $n=9$ ,  $p<0.002$ ) and 85% ( $n=4$ ,  $p<0.0001$ ) compared to untreated controls. In contrast, of three independent normal specimens tested, engraftment levels for DMAPT treated cells were 144% ( $n=5$ ,  $p=0.178$ ), 166% ( $n=5$  mice,  $p=0.77$ ), and 65% ( $n=5$ ,  $p=0.06$ ) relative to untreated controls, with no changes reaching statistical significance (representative example shown in Figure 2B). Together, these data indicate that DMAPT specifically ablates AML stem and progenitor cells without affecting the growth or engraftment potential of normal primitive cells.

## **DMAPT treatment induces stress responses, inhibits NF- $\kappa$ B, and activates p53**

We have previously shown that induction of oxidative stress, inhibition of NF- $\kappa$ B, and activation of p53 are functions associated with anti-LSC activity in primary AML cells.<sup>7</sup> In addition, we have identified prevalent pathways and genes affected by PTL using global gene expression analysis of CD34+ primary AML specimens (Hassane et al, manuscript in preparation). These experiments have identified strong up-regulation of NF-E2-related factor 2 (Nrf-2) and its transcriptional target heme oxygenase 1 (HO-1) in response to PTL treatment. Both genes are part of a cytoprotective response against oxidative stress,<sup>21</sup> and provide potential biomarkers for PTL-based drug responses. To evaluate the molecular consequences of DMAPT treatment, we first examined changes in oxidative stress using the reactive oxygen species (ROS) dye H2DCF-DA (DCF) and

the free thiol reactive dye mBBBr. As shown in Figure 3A, an increase in ROS levels and a decrease in free thiols were observed after as little as 15 minutes exposure of primary AML cells to DMAPT. The change in these two parameters indicates a rapid depletion of thiols and burst of ROS. Subsequent analysis of stress response mechanisms showed that HO-1 levels increase after 2 hours of treatment (Figure 3B), indicating that DMAPT is invoking a protective stress response against oxidative stress in the cell (n=3). A strong induction of Nrf2 nuclear localization was also observed (data not shown). Interestingly, inhibition of NF- $\kappa$ B occurs more slowly, with some decrease evident within an hour, but maximal reduction is not apparent until 4-8 hours (Figure 3C). Similarly, activation of p53, as detected by phosphorylation at ser15, is not evident until after approximately 8 hours of treatment. Notably, the anti-leukemia effect of DMAPT on AML cells becomes non-reversible only after 8 or more hours of exposure (data not shown), suggesting that changes in NF- $\kappa$ B and p53 may represent final (or late) steps in the commitment to cell death process. Together, these data indicate that DMAPT induces a rapid induction of oxidative stress followed by a series of cellular responses that include downstream stress control proteins and modulation of both survival and tumor suppressor mechanisms. These findings are in good agreement with previous hypotheses on the mechanisms that regulate selective targeting of LSC.<sup>10</sup>

### **DMAPT Pharmacology**

To further characterize the potential utility of DMAPT, preliminary pharmacological studies were performed. Not surprisingly, substantial pharmacokinetic (PK) differences were observed in rodent and canine studies. In mice, an oral DMAPT dose of 100mg/kg achieved a C<sub>max</sub> of 25  $\mu$ M and a half-life ( $T_{1/2}$ ) of 0.63 hours in serum. In contrast, canine studies showed a C<sub>max</sub> of 61  $\mu$ M, with a  $T_{1/2}$  of 1.9 hours when DMAPT was dosed at 100 mg/kg p.o. For both the mouse and canine models, oral bioavailability was approximately 70% in comparison to intravenous administration. These characteristics represent a significant improvement over PTL, which demonstrated a maximum serum concentration of 200 nM in mice when dosed at 40 mg/kg, which is the highest dose attainable given the relative insolubility of PTL.<sup>18</sup> Furthermore, in preliminary toxicology studies, daily administration of 100 mg/kg

DMAPT to mice for 10 consecutive days was well tolerated with no evidence of acute toxicity or changes in hematologic parameters. Similarly, daily oral dosing of dogs at 50-100 mg/kg for 14 consecutive days was well tolerated. Collectively, these studies indicate that the pharmacological properties of DMAPT are superior to PTL.

### ***In vivo* biological activity of DMAPT in a murine model**

Increased oxidative stress and inhibition of NF- $\kappa$ B are consistent *in vitro* features of DMAPT treatment (Figure 3 panels A, B and C). Thus, we tested whether such responses were also evident *in vivo* where they could serve as potential biomarkers for DMAPT activity. To this end, we injected primary human AML cells into sub-lethally irradiated NOD/SCID mice to establish xenografts. At 6 weeks post-injection (a time at which the AML cells have strongly engrafted in bone marrow), mice were treated with a single oral dose of 100mg/kg DMAPT. One hour post-treatment, animals were sacrificed to evaluate the bioactivity of DMAPT in human AML cells isolated from the bone marrow. Figure 3D shows that the NF- $\kappa$ B p65 subunit (yellow) is localized to the cytoplasm upon drug treatment (nucleus shown in blue), an activity indicating substantial inhibition of NF- $\kappa$ B (n=3). In addition, figure 3E shows that Nrf2 (green) localized to the nucleus, indicating its typical activation in response to oxidative stress (n=3). Together, these data indicate that DMAPT induces both the activation of stress responses and inhibition of NF- $\kappa$ B *in vivo*, and that both of these measurements can be used as biomarkers to monitor drug activity.

### ***In vivo* biological activity of DMAPT in spontaneous canine leukemias**

Spontaneous leukemias are well documented in dogs, and thus provide a large animal system in which to investigate drug activities. Therefore, we employed studies of primary canine leukemia as a means to further characterize the activity of DMAPT. First, *in vitro* studies were conducted to examine whether NF- $\kappa$ B is constitutively active in canine leukemias and whether such cells are sensitive to DMAPT. Constitutive NF- $\kappa$ B activity (as measured by EMSA) was evident in 5 out of 6 specimens tested (data not shown). Further, *in vitro* exposure to DMAPT for 24 hours resulted in decreased NF- $\kappa$ B activity (data not shown) as well as decreased cell survival (36% mean viability

at 10 $\mu$ M, n=6).

After establishing that DMAPT had similar effects in canine leukemia as human cells *in vitro*, we proceeded to test the *in vivo* biological activity of DMAPT by treating dogs with spontaneous leukemias. Notably, canine leukemias are usually only detected at advanced stages, where dogs diagnosed with acute disease have a median time to death of approximately 16 days. Furthermore, while the clinical profile of canine leukemia is similar to human disease, no information is available on LSC in the canine system. Therefore, these studies were not intended to determine whether DMAPT could target LSC *in vivo*, but rather provide a large animal model in which to assess basic parameters of drug activity. Case studies were performed in two dogs diagnosed with spontaneous leukemia:

Case study I was performed on an 8-year old male dog with a CD34+ acute leukemia in advanced stages of disease. The animal was treated for three consecutive days by oral gavage with increasing concentrations of DMAPT (50 mg/kg day 1, 75 mg/kg day 2 and 100 mg/kg day 3). Five days later (day 8), the dog received a second cycle of DMAPT administered at 75mg/kg for 4 consecutive days (skipping day 9). In addition, the animal received several supportive care measures including prednisone treatment (see methods). Figure 4A shows that DMAPT treatment decreased the levels of CD34 expression in peripheral leukemia cells, with notable reductions beginning at day 5. Moreover, after starting the second course of DMAPT treatment, CD34 expression decreased further. While no reductions in overall WBC were observed during the treatment period, the loss of CD34 expression indicates biological activity of DMAPT. The animal died at day 13 due to the advanced nature of his disease, but a bone marrow sample was obtained immediately post-mortem. Comparison to the pretreatment marrow specimen showed a strong reduction in CD34 expression for leukemic blasts (Figure 4B), indicating that the effects of DMAPT treatment were similar for marrow-resident vs. peripheral cells. Notably, analysis of p65 subcellular localization in cells derived from day 3 of treatment showed clear evidence of NF- $\kappa$ B inhibition *in vivo* (Figure 4C).

Case study II was performed on an 8-year old dog also diagnosed with a CD34+ acute leukemia. The dog was treated with oral DMAPT (50mg/kg) for 5 consecutive days. As observed with the first study, CD34 surface expression decreased (approximately 2-fold, figure 5A) while the WBC levels increased 1.5 fold. When the animal was left untreated for 10 subsequent days, the CD34 expression returned to levels observed at day 1, and the WBC continued to rise. A second round of treatment was then initiated at day 15 in which intravenous administration (i.v.) of DMAPT was employed at 50mg/kg. Since the C<sub>max</sub> for DMAPT i.v. is approximately double that of oral delivery, we reasoned that the higher C<sub>max</sub> might extend the duration of the physiologically relevant dose level and thereby provide improved bioactivity. As observed for the first course of treatment, CD34 levels decreased substantially and were accompanied by a parallel decrease in WBC. Over the same time frame an increase in peripheral neutrophils was also observed (figure 5C), suggesting that increased differentiation of tumor cells occurred. While the reduction in WBC may have been influenced by simultaneous supportive care treatment (30 mg of prednisone and clavamox on day 15), the data suggest a role for DMAPT in reducing tumor burden. Finally, as observed in Figure 4, DMAPT treatment resulted in both the induction of stress responses and inhibition of NF- $\kappa$ B (Figure 5B). Together, the data strongly suggest that DMAPT has significant *in vivo* bioactivity and can mediate several biological changes in primary leukemia cells that are consistent with *in vitro* biomarkers of AML-specific drug activity.

### **In vitro differentiation potential of DMAPT**

The findings from case study II suggested that DMAPT might induce differentiation of leukemia cells in certain situations. To further investigate this issue, U937 myelomonocytic cells were employed to test the *in vitro* differentiation potential of DMAPT. The U937 line is known to up-regulate CD11b and decrease growth in response to agents such as all-trans-retinoic acid (ATRA), and is a commonly employed system for assessing myeloid differentiation.<sup>22</sup> Figure 6 shows relative expression levels of CD11b on U937 cells cultured for 72 hours in the presence of ATRA or DMAPT. This cell line requires 20  $\mu$ M DMAPT to achieve high levels of cytotoxicity at

24h. Thus, the 2.5 and 5.0  $\mu\text{M}$  doses tested are well below the concentration needed to induce rapid cell death. Interestingly, while not as potent as ATRA, DMAPT treatment yielded a significant increase in CD11b expression, suggesting that this compound can act to induce myeloid differentiation.

## Discussion

*In vivo* targeting of LSCs represents a formidable challenge to the leukemia research field. Not only must future therapies more effectively eradicate LSCs, they must do so with less collateral damage to normal tissues. Several biological features of normal stem cells are retained in malignant populations and likely contribute to the difficulty in targeting the LSC population. For example, a mostly quiescent cell cycle status, expression of xenobiotic efflux pumps, and a protective microenvironmental niche are all factors that may shield LSC from therapeutic insult.<sup>23</sup> Thus, these parameters and possibly other aspects of *in vivo* biology must be considered for the development of improved regimens.

From basic studies of primary human tissue we have previously proposed that two types of events are necessary to induce preferential induction of cell death in LSCs: (i) inhibition of survival signals (such as NF- $\kappa$ B) and (ii) activation of stress responses.<sup>17</sup> Importantly, neither of these events alone appears to mediate substantial killing of LSC.<sup>16</sup> We hypothesize that stress responses such as increased activity of heat shock proteins, DNA damage pathways, and the phase II factors (i.e. HO-1 and Nrf2), are a direct result of drug-induced cellular damage and that increased NF- $\kappa$ B is a protective reaction to the insult. Thus, by inhibiting elements of the NF- $\kappa$ B pathway (or similar survival factors) the detrimental effects of stress, such as increased oxidative load, are uncovered by regimens that mediate both effects. We further hypothesize the PTL-based drugs fall into this class of drug, in which both induction of stress and inhibition of survival signals are central to the therapeutic mechanism.

In the present report, we have enhanced the anti-leukemia features of PTL, by creating a more pharmacologically useful form of the drug, DMAPT; and demonstrating that the analog retains key properties of the parent molecule. *In vitro* treatment of primary human AML, ALL and CML cells with DMAPT demonstrated potent eradication of leukemic stem and progenitor cells, as well as the overall blast population (Figure 1). Importantly, functional assays demonstrated that DMAPT specifically ablated primitive human leukemia cells without impairing their normal counterparts. Together, these data indicate DMAPT is a novel therapeutic candidate for targeting human LSCs, and may have utility against a broad range of hematologic cancers.

The findings above provide a strong rationale for taking DMAPT forward to human clinical trials for leukemia. However, we were cognizant that further characterization of the drug in some type of preclinical scenario could also be of value. While numerous studies have employed human-mouse xenografts to study biological properties of stem cells *in vivo*, there has been almost no use of such systems for therapeutic modeling. Indeed, the metabolic differences between mouse and human physiology make pharmacological comparisons difficult. Thus, our xenograft experiments were limited to relatively simple single-dose pharmacodynamic studies. In order to derive data more pertinent to human disease, we extended our *in vivo* studies to include analysis of spontaneous acute leukemia in dogs. While the study of canine disease is attractive because it provides a unique means to investigate authentic leukemia in a large animal system, it is also challenging due to the advanced stage in which disease is typically detected. Thus, the window of opportunity for treatment and evaluation is very brief. Nonetheless, we were able to conduct two case studies, roughly equivalent to human phase I clinical trials, in which pilot feasibility and pharmacodynamic analyses were performed (Figures 4-5). The findings from those studies indicate clear *in vivo* activity of DMAPT, as assessed by two independent biomarkers, in good agreement with previous data from *in vitro* studies and the mouse xenograft model. In addition, we also observed biological changes in tumor cells suggestive of drug efficacy. In both treated animals, a rapid decrease in the percentage of CD34+ cells was detected. Although the treatment and observation period was too short to determine whether sustained

changes could be maintained, this finding suggests either cytotoxicity to the leukemic cells and/or a strong induction of differentiation. Moreover, in case study II, the second course of drug treatment (administered i.v.) mediated a substantial reduction in tumor volume and an increase in differentiated cells found in peripheral circulation, again indicating cytotoxicity and/or differentiation of leukemic cells. Subsequent *in vitro* studies further supported the concept that DMAPT can cause differentiation prior to induction of cell death (Figure 6), a finding consistent with the *in vivo* data.

Taken together, the data indicate that DMAPT mediates *in vivo* biological changes in leukemia cells that will lead to their impairment and/or death. Moreover, given the strong efficacy of the drug for AML stem and progenitor cells *in vitro*, we propose that a similar effect is possible *in vivo*. Based on these preclinical studies, and a favorable toxicology profile, DMAPT is proceeding to human phase I clinical trials in the near future.

## Acknowledgements

We dedicate this manuscript in loving memory of Isaac Greenlaw, whose spirit lives on through his contributions to our work.

We sincerely thank Dr. Timothy Bushnell for expert advice in flow cytometry and Dr. Anne Avery for assistance with canine pathology studies. We gratefully acknowledge support from the Douglas Kroll research foundation, the Leukemia and Lymphoma Society (6099-06), the National Cancer Institute (R01CA90446), and the US Dept of Defense (DAMD17-03-1-0263). CTJ is a Scholar of the Leukemia and Lymphoma Society. Pharmacology studies were supported in part through the NCI-RAID Program of the Developmental Therapeutics Program, Division of Cancer Treatment and Diagnosis, National Cancer Institute, National Institutes of Health. The content of this publication does not necessarily reflect the views or policies of the Department of Health and Human Services nor does mention of trade names, commercial products, or any organization imply endorsement by the U.S. Government.

**Author contributions:** M.L.G. designed research, performed research, analyzed data, and helped write the paper. R.M.R. performed research. S.N. designed research, performed research, and analyzed data. X.L. performed research. C.C. performed research. D.C.H. performed research and analyzed data. M.W.B. performed research and analyzed data. J.M.B. analyzed data. E.S. performed research and analyzed data. J.L.L. performed research. C.J.S. contributed vital reagents and analyzed data. W.M. analyzed data and helped write the paper. M.C. contributed vital reagents and analyzed data. J.L.L. contributed vital reagents. P.A.C. designed research and analyzed data. C.T.J. designed research, analyzed data, and helped write the paper.

## References

1. Bonnet D, Dick JE. Human acute myeloid leukemia is organized as a hierarchy that originates from a primitive hematopoietic cell. *NatMed*. 1997;3:730-737.
2. Lapidot T, Sirard C, Vormoor J, et al. A cell initiating human acute myeloid leukaemia after transplantation into SCID mice. *Nature*. 1994;367:645-648.
3. Cox CV, Evely RS, Oakhill A, Pamphilon DH, Goulden NJ, Blair A. Characterization of acute lymphoblastic leukemia progenitor cells. *Blood*. 2004;104:2919-2925.
4. Holyoake T, Jiang X, Eaves C, Eaves A. Isolation of a highly quiescent subpopulation of primitive leukemic cells in chronic myeloid leukemia. *Blood*. 1999;94:2056-2064.
5. Graham SM, Jorgensen HG, Allan E, et al. Primitive, quiescent, Philadelphia-positive stem cells from patients with chronic myeloid leukemia are insensitive to STI571 in vitro. *Blood*. 2002;99:319-325.
6. Guan Y, Gerhard B, Hogge DE. Detection, isolation, and stimulation of quiescent primitive leukemic progenitor cells from patients with acute myeloid leukemia (AML). *Blood*. 2003;101:3142-3149.
7. Guzman ML, Rossi RM, Karnischky L, et al. The sesquiterpene lactone parthenolide induces apoptosis of human acute myelogenous leukemia stem and progenitor cells. *Blood*. 2005;105:4163-4169.
8. Killmann SA. Acute leukaemia: development, remission/relapse pattern, relationship between normal and leukaemic haemopoiesis, and the 'sleeper-to-feeder' stem cell hypothesis. *Baillieres Clin Haematol*. 1991;4:577-598.
9. van Rhenen A, Feller N, Kelder A, et al. High stem cell frequency in acute myeloid leukemia at diagnosis predicts high minimal residual disease and poor survival. *Clin Cancer Res*. 2005;11:6520-6527.
10. Jordan CT, Guzman ML. Mechanisms controlling pathogenesis and survival of leukemic stem cells. *Oncogene*. 2004;23:7178-7187.
11. Jordan CT, Upchurch D, Szilvassy SJ, et al. The interleukin-3 receptor alpha chain is a unique marker for human acute myelogenous leukemia stem cells. *Leukemia*. 2000;14:1777-1784.
12. Guzman ML, Upchurch D, Grimes B, et al. Expression of tumor-suppressor genes interferon regulatory factor 1 and death-associated protein kinase in primitive acute myelogenous leukemia cells. *Blood*. 2001;97:2177-2179.
13. Guzman ML, Neering SJ, Upchurch D, et al. Nuclear factor-kappaB is constitutively activated in primitive human acute myelogenous leukemia cells. *Blood*. 2001;98:2301-2307.
14. Mayo MW, Baldwin AS. The transcription factor NF-kappaB: control of oncogenesis and cancer therapy resistance. *Biochim Biophys Acta*. 2000;1470:M55-62.
15. Nakanishi C, Toi M. Nuclear factor-kappaB inhibitors as sensitizers to anticancer drugs. *Nat Rev Cancer*. 2005;5:297-309.
16. Guzman ML, Swiderski CF, Howard DS, et al. Preferential induction of apoptosis for primary human leukemic stem cells. *Proc Natl Acad Sci U S A*. 2002;99:16220-16225.

17. Guzman ML, Jordan CT. Considerations for targeting malignant stem cells in leukemia. *Cancer Control*. 2004;11:97-104.
18. Sweeney CJ, Mehrotra S, Sadaria MR, et al. The sesquiterpene lactone parthenolide in combination with docetaxel reduces metastasis and improves survival in a xenograft model of breast cancer. *Mol Cancer Ther*. 2005;4:1004-1012.
19. Lansdorp PM, Dragowska W. Long-term erythropoiesis from constant numbers of CD34+ cells in serum-free cultures initiated with highly purified progenitor cells from human bone marrow. *JExpMed*. 1992;175:1501-1509.
20. Topisirovic I, Guzman ML, McConnell MJ, et al. Aberrant eukaryotic translation initiation factor 4E-dependent mRNA transport impedes hematopoietic differentiation and contributes to leukemogenesis. *Mol Cell Biol*. 2003;23:8992-9002.
21. Jeong WS, Jun M, Kong AN. Nrf2: a potential molecular target for cancer chemoprevention by natural compounds. *Antioxid Redox Signal*. 2006;8:99-106.
22. Caprodossi S, Pedinotti M, Amantini C, et al. Differentiation response of acute promyelocytic leukemia cells and PML/RAR $\alpha$  leukemogenic activity studies by real-time RT-PCR. *Mol Biotechnol*. 2005;30:231-238.
23. Jordan CT, Guzman ML, Noble M. Mechanisms of Disease. *Cancer Stem Cells*. *The New England Journal of Medicine*. 2006;355:55-66.

## Figure Legends.

**Figure 1. DMAPT induces death of primary human AML, ALL and CML cells but not normal hematopoietic cells.** (A) Percent viability of primary human AML cells exposed to either 7.5 $\mu$ M PTL or DMAPT. Viability was measured by labeling with Annexin V and 7-AAD. Analysis of total AML vs. selected CD34<sup>+</sup> cells are indicated. (B) Percent viability of CD34<sup>+</sup>CD38<sup>-</sup> AML cells at the indicated concentrations of DMAPT. (C) Percent viability of CD34<sup>+</sup>CD10<sup>-</sup> ALL cells at the indicated concentrations of DMAPT. (D) Percent viability on CD34<sup>+</sup>CD38<sup>-</sup> CML cells at the indicated concentrations of DMAPT. (E) Percent viability of normal CD34<sup>+</sup> or CD34<sup>+</sup>CD38<sup>-</sup> hematopoietic cells obtained from healthy donors (CB or BM) and treated at the indicated concentrations of DMAPT. In all panels the horizontal bars represent the mean and each circle or diamond represents one specimen. Analysis of each specimen was performed in triplicate and the average was used to represent the results for a single specimen. All viability values are relative to untreated controls.

**Figure 2. Progenitor/stem cell functional assays for DMAPT treated cells.** (A) AML versus normal cells were treated with 5  $\mu$ M DMAPT for 18 hours in suspension culture, followed by plating in methylcellulose culture. Horizontal bar represents the mean. \*\*  $p < 0.001$  AML vs. erythroid and AML vs. myeloid. The percent of colony-forming units (CFU) was normalized to untreated control. All assays were performed in triplicate. (B) Representative examples of the percent engraftment achieved in NOD/SCID mice receiving AML (left panel) or normal CB (right panel) cells after 18 hours of culture with or without 7.5  $\mu$ M DMAPT. Each symbol represents a single animal analyzed at 6 to 8 weeks after transplantation. Mean engraftment is indicated by the horizontal bar. \*\*\*  $p < 0.0001$  DMAPT vs. untreated (UNT).

**Figure 3. DMAPT induces stress responses and inhibits NF- $\kappa$ B.** (A) Relative fold change on linear scale for DCF (left panel) and mBBr (right panel) after the indicated time (x-axis) of treatment with DMAPT. (B) Confocal micrograph of primary human AML cells with treated with 7.5 $\mu$ M DMAPT for 2 hours. HO-1 (green) and nucleus (ToPro3,

represented in red). (C) Immunoblots (top two panels) for phospho p53ser15 (top) or actin (middle) of CD34+ primary human AML cells treated with 7.5 $\mu$ M DMAPT for the indicated times. Bottom panel shows an EMSA for NF- $\kappa$ B binding for the same treatment. (D and E) NOD/SCID mice engrafted with human AML cells 6 weeks prior to the experiment were treated with a single i.p. dose of 100mg/kg DMAPT or saline control. One hour later animals were sacrificed and BM was harvested and analyzed by confocal microscopy. Panel D shows NF- $\kappa$ B (p65 subunit in yellow) and panel E shows Nrf-2 (green). The nucleus is shown in blue for both panels.

**Figure 4. Spontaneous canine CD34+ leukemia: Case study I.** (A) Percent CD34 cell surface expression was examined from PB samples obtained at the indicated day and is represented by the open bars. Dashed line represents the WBC (x1000/ $\mu$ l) for the same sample. (B) Flow cytometric plot showing PB (top panels) or BM (bottom panels) cells obtained at the indicated days of DMAPT treatment (D0=pre-treatment, D4= day 4, D5= day 5, D13= day 13). Y-axis shows CD34-PE and X-axis shows CD45-FITC. (C) Confocal micrograph for canine cells obtained from day 3. Pre (left panel) shows cells before the animal received the treatment, and post (right panel) shows the cells 4 hours after the treatment with 100mg/kg DMAPT

**Figure 5. Spontaneous canine CD34+ leukemia: Case study II.** (A) Percent CD34 cell surface expression was examined from PB samples obtained at the indicated day and is represented by the open bars. Dashed line represents the WBC (x1000/ $\mu$ l) for the same sample. (B) Confocal micrograph for canine cells obtained before treatment (day 0) or from day 5 after initial treatment with 50mg/kg oral dose DMAPT. Top panels show cells stained for NF- $\kappa$ B p65 (yellow) and ToPro3 (blue). Bottom panels show  $\gamma$ H2AX (green) and ToPro3 (red). (C). Blood smears for PB samples obtained at the indicated days. Arrow shows neutrophils.

**Figure 6. U937 differentiation assay for DMAPT treatment.** Percent CD11b expression after 72 hours treatment with sublethal concentrations of DMAPT. ATRA

treatment is shown as control. Horizontal line represents CD11b levels in untreated control cells. \*\*  $p < 0.001$

**Leukemia stem cells in a genetically defined murine  
model of blast crisis CML**

Sarah J. Neering<sup>1</sup>, Timothy Bushnell<sup>1,2,\*</sup>, Selcuk Sozer<sup>3,\*</sup>, John Ashton<sup>4</sup>, Randall M. Rossi<sup>1</sup>, Pin-Yi Wang<sup>5</sup>, Deborah R. Bell<sup>6</sup>, David Heinrich<sup>7</sup>, Andrea Bottaro<sup>1,7,8</sup>, and Craig T. Jordan<sup>1,2,7,#</sup>

<sup>1</sup> James P. Wilmot Cancer Center, University of Rochester Medical Center, 601 Elmwood Avenue, Rochester, NY, 14642.

<sup>2</sup> Center for Pediatric Biomedical Research, University of Rochester Medical Center, 601 Elmwood Avenue, Rochester, NY, 14642.

<sup>3</sup> Dept. of Microbiology and Immunology, University of Kentucky, 800 Rose Street, Lexington, KY, 40536 (present address: Dept. of Hematology/Oncology, University of Chicago, 909 S. Wolcott Street, Chicago, IL, 60612)

<sup>4</sup> Dept. of Biomedical Genetics, University of Rochester School of Medicine, 601 Elmwood Avenue, Rochester, NY, 14642.

<sup>5</sup> Dept. of Pathology, University of Rochester Medical Center, 601 Elmwood Avenue, Rochester, NY, 14642.

<sup>6</sup> Markey Cancer Center, University of Kentucky, 800 Rose Street, Lexington, KY, 40536 (present address: Eli Lilly Inc., Indianapolis, IN, 46285)

<sup>7</sup> Dept. of Medicine, University of Rochester School of Medicine, 601 Elmwood Avenue, Rochester, NY, 14642.

<sup>8</sup> Dept. of Microbiology and Immunology, University of Rochester School of Medicine, 601 Elmwood Avenue, Rochester, NY, 14642.

\* These authors contributed equally.

#Corresponding author:

Craig T. Jordan, PhD  
University of Rochester Medical Center  
601 Elmwood Ave, Box 703  
Rochester, NY, 14642  
Telephone: 585-275-6339  
Email: craig\_jordan@urmc.rochester.edu

Text word count: 4605

Abstract word count: 196

Running Title: leukemia stem cell model

Category: Neoplasia

## **Abstract**

Myeloid leukemia arises from leukemia stem cells (LSC), which are resistant to standard chemotherapy agents and likely to be a major cause of drug resistant disease and relapse. To investigate the in vivo properties of LSC, we developed a mouse model in which the biological features of human LSC are closely mimicked. Normal hematopoietic stem cells (HSC) were modified to express the BCR/ABL and Nup98/HoxA9 translocation products and a distinct LSC population, with the aberrant immunophenotype of lineage-, Kit<sup>+/</sup>, Flt3+, Sca+, CD34+, and CD150-, was identified. In vivo studies were then performed to assess the response of LSC to therapeutic insult. Treatment of animals with the ABL kinase inhibitor imatinib mesylate induced specific modulation of blasts and progenitor cells but not stem cell populations, thereby recapitulating events inferred to occur in human CML patients. In addition, challenge of leukemic mice with total body irradiation was selectively toxic to normal HSC, suggesting that LSC are resistant to apoptosis and/or senescence in vivo. Taken together, the system provides a powerful means by which the in vivo behavior of LSC vs. HSC can be characterized and candidate treatment regimens can be optimized for maximal specificity towards primitive leukemia cells.

## Introduction

A broad range of studies indicates that chronic and acute forms of human myelogenous leukemia arise from mutations occurring at the hematopoietic stem or progenitor cell level. These reports show that LSC share many properties of normal HSC, including a distinct immunophenotype, relatively quiescent cell cycle status, and low frequency <sup>1-6</sup>. In addition, LSC possess the canonical stem cell properties of self-renewal, multipotentiality, and strong proliferative capacity <sup>7-9</sup>. Thus, the organization of leukemic populations appears to mirror the hierarchical structure of normal hematopoietic tissues, with a central stem cell driving the overall system. Consequently, from a biological and therapeutic perspective, characterizing the leukemia stem cell is key to understanding leukemia pathogenesis and for developing more effective therapeutic regimens <sup>10-12</sup>.

In order to study the *in vivo* biology of LSC, several recent studies have begun to characterize the genesis of malignant stem cells in different murine models <sup>13-16</sup>. These studies have shown that hematopoietic stem cells as well as various progenitors can serve as targets for leukemic transformation. Further, while details vary depending on the specific mutations and experimental procedures employed, recent reports have also shown that phenotypically identifiable and functionally distinct LSC can be found in murine models <sup>15,17,18</sup>, thereby validating the mouse as a useful system in which to study LSC. To date, murine studies of LSC have employed expression of a single mutation, which induces subsequent evolution of acute disease with varying kinetics. To generate a more defined genetic system, we have employed previously described manipulations involving well known leukemia mutations. Beginning with the studies of Daley et al in 1991 <sup>19</sup>, it has been known that expression of the BCR/ABL translocation in murine marrow cells is sufficient to induce a model of chronic phase CML <sup>20</sup>. More recently, studies have demonstrated that simultaneous expression of an appropriate second mutation leads to an acute form of disease that resembles blast crisis CML (bcCML) <sup>21-23</sup>. Importantly, such “two hit” systems appear to be genetically sufficient to induce disease, and thus provide a defined background in which biological studies may be performed. For the studies presented herein, we have pursued a model that employs retroviral vectors to co-express the BCR/ABL and Nup98/HoxA9 translocation products <sup>22,23</sup>. These two mutations have previously been documented in leukemia patients <sup>24,25</sup>, thereby corroborating the relevance

of these particular genetic aberrancies to human disease. Further, the nature of the translocations is consistent with proposed theories on the molecular genetics of acute leukemia in which the combination of a strong mitogenic signal (i.e. constitutive kinase activation such as seen with BCR/ABL, Flt3, Jak2, etc) along with mutations that inhibit differentiation (e.g. transcription factor-based anomalies such as Nup98/HoxA9, AML1-ETO, etc) are key components of transformation <sup>26</sup>. Indeed, based on the biology of the system, interaction between BCR/ABL and Nup98/HoxA9 appears to fulfill the criteria for true oncogene cooperativity.

Our findings in the BCR/ABL and Nup98/HoxA9 system indicate that LSC are relatively rare, possess a distinct cell surface immunophenotype, and retain physiological and homeostatic mechanisms reminiscent of normal stem cell based hematopoietic populations. Moreover, the consequences of drug or radiation challenge can be readily ascertained and appear to recapitulate physiological responses one might expect from human LSC in vivo. Therefore, we propose that the model provides a platform from which the properties of normal vs. malignant stem cells can be examined and that the relative effects of therapeutic regimens can be evaluated in vivo.

## Materials and Methods

### Plasmids and virus production

The MSCV-BCR/ABL-IRES-GFP vector was kindly provided by Dr. Richard Van Etten. The MSCV-Nup98/HoxA9-NEO plasmid was kindly provided by Dr. Guy Sauvageau. The neo gene was removed from this vector by digestion with Nco I and Cla I, and the YFP gene was inserted by standard cloning procedure to yield the MSCV-Nup98/HoxA9-YFP vector used in the present study. Retroviral vector plasmids were transfected into phoenix-eco cells (ATCC) using lipofectamine 2000 per manufacturer's instructions (10 micrograms DNA per 100,000 cells in a six-well tissue culture dish). At 36 hours post-transfection, viral supernatants were collected, filtered, and stored at -80 degrees centigrade.

### Generation of animal models

Six to eight week old female C57BL6/J mice were purchased from JAX or the NCI. Donor animals were sacrificed and marrow was flushed from femurs and tibias. Single cell suspensions were depleted of lin<sup>+</sup> cells using BD IMag<sup>TM</sup> immunoaffinity system per manufacturer's instructions. Purified populations of HSC, CMP, and GMP were isolated as described below. Donor cell populations were plated in 24-well dishes coated with retronectin (Takara) (day 1) and cultured overnight in IMDM containing SCF (25ng/ml), Flt3 (25ng/ml), IL3 (10ng/ml), and IL3 (10ng/ml). The following day (day 2), 50% of culture media was replaced with viral supernatant, once in the morning, and again in the evening. The viral infection procedure was repeated again on day 3. On the morning of day 4, cells were harvested, resuspended in cold PBS, and injected IV into recipient C57BL6/J mice. For the CML model (i.e. BCR/ABL alone), recipient animals were sublethally irradiated (600 rads) to facilitate engraftment. For the blast crisis model (BCR/ABL + Nup/98), no irradiation was required.

### Flow cytometry and phenotyping

For phenotyping of major lineages (Table 1), marrow cells were labeled with antibodies to red cell precursors (Ter119), B cells (B220), T cells (CD3), myeloid cells (Gr-1), or a cocktail of all lineage-specific markers (Lin) (all antibodies from Becton Dickinson). For sorting experiments, lineage depleted (lin<sup>-</sup>) bone marrow cells were labeled with antibodies

to Sca-1, CD34, Flt3, CD150, c-kit, and the Fc-gamma receptor (2.4G2) (all antibodies from Becton Dickinson) and sorted to isolate the desired subpopulations using a FACARIA™ flow cytometer and standard procedures. For cell cycle studies, antibody labeled populations were fixed in 1% ultrapure formaldehyde (Polysciences, Inc.) for 20 minutes and permeabilized with 0.1% Triton for 20 minutes. Fixed cells were then labeled with DAPI (5 ug/ml) and analyzed for DNA cycle profiles using FlowJo 8.2 software.

#### Southern blots

Genomic DNA from bone marrow was digested with EcoRI, separated by electrophoresis on 0.8% agarose Tris-acetate-EDTA gels and transferred onto GeneScreen Plus membranes (Perkin Elmer). Blots were sequentially hybridized with [<sup>32</sup>P]-labeled probes for EGFP, using the entire EGFP coding sequence from a pEGFP-C2 plasmid (Clontech Laboratories). The blots were washed at high stringency, and hybridization was detected after exposure onto Molecular Dynamics Phosphor Screens using a Storm 860 Imaging System scanner and ImageQuant software (Molecular Dynamics).

#### In vitro colony-forming assays

The indicated cell populations were plated in methylcellulose medium (Stem Cell Technologies, M3134) supplemented with 15% FBS, 20% BIT (BSA, insulin, transferin – Stem Cell Technologies, #09500), SCF (50 ng/ml), IL3 (10 ng/ml), Flt-3 (50 ng/ml), and IL6 (10 ng/ml). Cultures were incubated at 37 degrees centigrade for 10-14 days before scoring colonies (100 or more cells/colony).

#### In vivo studies

For drug challenge, cohorts of leukemic mice were established as described in the text. At advanced stages of disease, 100mg/kg of ara-C was administered by intraperitoneal injection. Animals were sacrificed 4 or 20 hours later and subjected to immunophenotyping and cell cycle analysis as described above. Alternatively, imatinib mesylate (100mg/kg in water) was administered by oral gavage twice daily for three consecutive days before mice were sacrificed and analyzed. For studies requiring pre-transplant conditioning, animals were exposed to 550 rads from a Rad Source 2000 X-ray irradiator. At 7 days post treatment, animals were sacrificed and analyzed as described.

## Results

### Model systems for chronic and blast crisis CML

Initial studies were performed to validate systems using both BCR/ABL alone (CML model) and in combination with Nup98/HoxA9 (bcCML model) to induce disease. For gene transfer retroviral vectors encoding each translocation product and a distinct fluorescent protein marker (GFP and YFP) were employed to allow delineation of cells transduced with one or both vectors. Enriched marrow stem cell populations from donor C57BL/6-Ly5.1 mice were infected with one or both vectors and transplanted into C57BL/6-Ly5.2 congenic recipients. Figure 1A shows a typical example of the resulting disease where expression of the GFP and YFP markers can be used to identify singly vs. doubly transduced populations. As noted by comparing boxes I-III, in primary recipients we detect cells transduced with either vector alone or in combination, whereas upon transfer to secondary recipients (Figure 1B), the more aggressive acute disease predominates. Figure 1B also verifies that expression of GFP and YFP accurately reflects the donor-host origin of cells in the model. Table 1 provides a comparison of naïve, control, CML, and bcCML models with respect to the frequencies of various lineages and populations. As expected, with disease progression an increase in both primitive (lineage negative, lin-) and myeloid cell types were observed, with a concomitant reduction in lymphoid cell types. The table also shows comparison of transduced (GFP+) vs. normal (GFP-) cells co-resident within in each model. As shown in Figure 2A, evolution of the CML-like disease typically requires 16-18 days to cause death, and is only manifest when naïve HSC are used as donor cells. As previously reported, transduction of myeloid progenitors (common myeloid progenitors, CMP; or granulocyte-monocyte progenitors, GMP) with BCR/ABL is not sufficient to induce disease<sup>14</sup>. In contrast, the bcCML disease develops more quickly, with advanced disease evident in as little as 10 days. Moreover, simultaneous expression of both translocations permits myeloid progenitors (CMP and GMP) to serve as targets for transformation, albeit with somewhat slower kinetics (Figure 2B). Notably, while transplantation of the CML disease requires sublethal irradiation of host animals (600 rads), bcCML was successfully transferred without any preconditioning regimen. Thus, for the experiments in this study no irradiation of host animals was required for the bcCML model. This finding indicates that LSC arising from the combined translocations are both quantitatively and qualitatively more aggressive than stem cells transduced with BCR/ABL alone.

Previous studies have shown that expression of BCR/ABL alone is sufficient to induce CML-like myeloproliferative disease, and that no additional mutations are required. This finding is based on the relatively rapid kinetics of disease formation, and the polyclonal nature of malignant cells arising *in vivo* <sup>27</sup>. Similarly, the bcCML form of disease also appears to arise directly from expression of BCR/ABL + Nup98/HoxA9, without requiring additional mutations. The pathogenesis is extremely rapid and leukemic animals display a highly polyclonal disease profile (Figure 3). Moreover, animals within the same cohort display distinct retroviral integration patterns, indicating the presence of multiple independent clones sufficient to mediate disease. Thus, combination of BCR/ABL + Nup98/HoxA9 provides a genetically defined background in which to explore the features of leukemia stem cells. We note that during pathogenesis of human disease acquisition of the two mutations would typically occur in a sequential rather than simultaneous fashion. Therefore, primary animals were established expressing BCR/ABL-GFP alone. Lin-marrow derived from these animals was then harvested and used for transduction with the Nup98/HoxA9 virus. Upon transplantation into secondary recipients, the sequentially infected cells generated a bcCML disease that was indistinguishable from the model generated by simultaneous infection (data not shown).

### Leukemia Stem Cell Phenotype

To identify the leukemia-initiating cell for the chronic and blast crisis models, we infected purified HSC with one or both vectors, transplanted naïve recipients, and isolated leukemic cells from primary mice in advanced stages of disease. Bone marrow from such animals was labeled with a range of antibodies (myeloid, T cell, B cell, and erythroid – see methods), sorted to purify specific subpopulations, and transplanted into secondary recipient mice to assess leukemic potential. For the chronic phase model, we first separated lin<sup>+</sup> vs. lin<sup>-</sup> cells and determined that all detectable leukemia-initiating activity was in the lin<sup>-</sup> cells (two independent experiments, n = 15 mice). Subsequent fractionation of the lin<sup>-</sup> population into lin<sup>-</sup>/kit<sup>+</sup> vs. lin<sup>-</sup>/kit<sup>-</sup> showed all leukemic potential in the Lin<sup>-</sup>/kit<sup>+</sup> cells (three independent experiments, n = 18 mice). Finally, comparison of Lin<sup>-</sup>/Kit<sup>+</sup>/Sca<sup>+</sup> vs. Lin<sup>-</sup>/kit<sup>+</sup>/Sca<sup>-</sup> indicated 100% of transplantable LSC activity was in the Lin<sup>-</sup>/Kit<sup>+</sup>/Sca<sup>+</sup> (three independent experiments, n = 18 mice). Thus, the CML LSC displays a phenotype similar to normal HSC (Figure 4), and only cells bearing the Lin<sup>-</sup>/Sca<sup>+</sup>/kit<sup>+</sup> phenotype were

able to generate disease in secondary recipients. Parallel studies of in vitro colony-forming ability were also performed and indicated that CFU potential is highly enriched in the Lin-/Sca+/kit+ population, as is observed for normal cells (Table 2). Therefore, the developmental and hierarchical structure of cells arising in chronic phase disease appears to be very similar to normal populations, both with regard to in vitro CFU and transplantation potential.

LSC for the bcCML model were defined using a series of sorting and limiting dilution experiments that included analysis of multiple markers associated with primitive stem and progenitor populations. We found that Lin+ cells contained only 1 in 1959 cells capable of initiating disease, a level consistent with the purity of transplanted populations. Thus, as observed for the chronic phase model, essentially all LSC reside in the Lin- compartment. Further fractionation of Lin- cells was undertaken using antibodies for several stem cell associated markers: Sca-1, c-kit, Flt3, CD150, CD34, and Fcγ receptor (III/II). Expression of Sca-1 was strongly associated with LSC activity, with approximately 87% of detectable potential in the Sca-1+/Lin- fraction in comparison to Sca-1-/Lin- cells. Similarly, Flt3 also correlated with LSC potential, with 82% of LSC in the Flt+/Lin- populations in comparison to Flt-/Lin- cells. In contrast, the HSC antigen CD150<sup>28</sup> was not strongly expressed on primitive leukemia cells, with 96% of LSC potential found in the Sca+/CD150-/Lin- population. By combining these markers, we observed that Sca+/Flt+/CD150-/Lin- cells contained 1 in 7 LSC by limiting dilution (two independent experiments, n=12 mice per experiment) and identified the majority of leukemia-initiating potential (Figure 4). Within this defined population, virtually all detectable cells were CD34+, thus the marker was not used for sorting strategies because it provided no further enrichment of LSC. Interestingly, c-kit was not a particularly useful marker for purification. Expression of c-kit is suppressed in bcCML leukemic cells, with the majority of the Lin- population possessing an intermediate level of antigen (Figure 4). Collectively, these antigenic features most closely resemble the phenotype of short-term HSC (ST-HSC) or possibly CMP, but are nonetheless aberrant and thereby distinguish the blast crisis LSC from normal HSC.

In vitro CFU assays in the bcCML model indicated less rigid developmental boundaries for primitive cells (Table 2). For example, while all the markers found on LSC were

associated with substantial CFU potential, there was also significant enrichment of colony-forming ability observed for the Lin-/Sca- and Lin-/Flt- populations. These data indicate that a feature of blast crisis disease may be significantly elevated levels of self-renewal/growth within various progenitor populations, a finding consistent with similar studies from human CML<sup>29</sup>.

### Cell cycle analyses

Cell cycle regulation is an important aspect of stem cell biology and is likely related to tissue homeostasis and relative sensitivity to chemotherapy drugs. We thus performed a detailed analysis of stem and progenitor populations in the CML models. A notable feature of the experimental system is that co-resident populations of normal vs. leukemic cell types can be analyzed within the same animal. In addition, appropriate non-leukemic control transplants were analyzed. Table 3 shows the results of multiparameter flow cytometry studies in which cell cycle rates and the frequency of various phenotypically defined subpopulations were determined. Several features of the data are worth noting. First, within the stem cell compartment of the chronic phase model, cycle rates are nearly double for GFP+ vs. GFP- cells. Thus, expression of BCR/ABL is strongly mitogenic and dramatically increases the growth rate of the stem cell compartment. However, despite the elevated cycle rate, the frequency of cells in the primitive compartment is very similar to normal stem cells. This finding indicates that self-renewal frequency is not altered and that normal homeostatic regulation of stem cell pool size is intact. Notably, elevated cycle rate but normal compartment size is also observed for progenitor cells in the chronic phase model. In contrast, co-expression of BCR/ABL + Nup98/HoxA9 creates a malignant stem cell population in which cell cycle rates are no different than normal stem cells. However, the relative frequency of bcCML LSC is elevated over 10-fold in comparison to GFP controls (0.3% vs. 0.02%), suggesting an increase in self-renewal, but relatively normal growth rates for stem cells in the blast crisis model. Taken together, these findings indicate that the pathogenic mechanisms by which chronic vs. acute forms of CML overwhelm normal hematopoiesis may be fundamentally different. The data also suggest that the consequences of drug treatment may vary substantially as a function of disease state and LSC cycle status.

### In vivo effects of leukemia drugs

To assess the in vivo biology of primitive cells with regard to drug insult, we first examined the agent Ara-C (cytosine arabinoside) as a model of conventional cytotoxic chemotherapy. For these studies, cohorts of non-irradiated mice were transplanted with BCR/ABL-GFP + Nup98/HoxA9-YFP infected cells from primary donors. At 10-11 days post-transplant, tumor burden was rapidly increasing (high WBC, splenomegaly, and ~25-50% leukemic cells in marrow), thus approximating advanced stages of human disease. Leukemic animals were then challenged with a single bolus of Ara-C (100 mg/kg), and sacrificed 4 or 20 hours later for analysis (n=3 animals per timepoint, two independent experiments). These two timepoints were chosen based on previous studies of normal HSC in which nadir and rebound of the stem cell compartment occurred at 4 and 20 hours post-treatment respectively <sup>30</sup>. As shown in Table 4, Ara-C has a significant and rapid effect on the stem cell compartment, with approximately 50% reduction in the cycling pool (S + G2 populations) within 4 hours. Notably, there is no significant difference between normal and leukemia stem cells, indicating the effects of Ara-C towards primitive cells are non-specific. By 20 hours, both populations have returned to near steady-state cycle levels, indicating an equivalent ability of normal vs. leukemic stem cells to respond to insult and recover following drug challenge. Similar effects were noted for the progenitor population.

In a parallel series of experiments, we examined the widely used CML drug imatinib mesylate as a model of non-toxic targeted therapy. For these studies, animals were again allowed to progress to advanced stages of disease and then treated for three consecutive days before sacrifice and analysis (Table 4, n=3 animals per timepoint, two independent experiments). Interestingly, treatment with imatinib has completely opposite effects on the stem vs. progenitor populations. The more primitive cells exhibit a modest decrease in cell cycle activity, suggesting that drug treatment is somewhat inhibitory towards stem cell growth rate, consistent with in vitro studies of human cells <sup>31</sup>. In contrast the progenitor pool shows a substantial increase in cycle rate, possibly indicating a homeostatic response to systemic pressure exerted by the effects of imatinib. As noted for Ara-C treatment, the relative effects on cell cycle rate are very similar between normal and leukemic populations. However, one notable leukemia-specific consequence of imatinib treatment was detected. Examination of the differentiation state of treated animals showed the

leukemic cells reduced the overall proportion of lin<sup>-</sup> cells by approximately 50%, with a concomitant increase in Lin<sup>+</sup> cells. Presumably, this shift represents increased differentiation of the leukemic population, an effect consistent with the known clinical effects of imatinib. Thus, increased cycling of progenitor cells may be a homeostatic response of the leukemic population to increased differentiation pressure. Importantly, elevated cycle rates of the progenitor pool suggest that at least short-term imatinib exposure was not inhibitory to primitive cells in vivo.

#### Response of normal vs. leukemic stem cells to irradiation

Finally, we examined treatments used for bone marrow transplantation (BMT) procedures. Prior to BMT, patients are commonly treated with total body irradiation as part of a conditioning regimen to ablate endogenous disease and enhance engraftment of donor hematopoietic cells. In many cases, patients undergoing such a procedure are in clinical remission. While this procedure is beneficial for engraftment of normal donor stem cells, the relative effects of irradiation on residual LSC are unknown. Moreover, radiation is known to impair the viability/function of normal endogenous HSC in the host<sup>32,33</sup>. Thus, we employed our model system to investigate relative effects of radiation on LSC vs. HSC in vivo. To this end, the system was modified to examine treatment of leukemic animals with low tumor burden. Cohorts of mice bearing the BCR/ABL + Nup98/HoxA9 leukemia were established as described above and challenged during early stages of disease (2-3 days post-transplant). At this phase of disease evolution, no leukemic cells are yet evident in peripheral circulation and marrow levels are extremely low. Thus, irradiation at this point is roughly equivalent to patients with minimal residual disease. At 7 days following irradiation, animals were sacrificed and analyzed with respect to stem and progenitor cell content (n=3 animals per group, two independent experiments). As shown in Figure 5A, while the percentage of phenotypically-defined normal HSC was dramatically reduced, the LSC populations were only modestly suppressed in comparison to non-irradiated controls. Similarly, the frequency of progenitor cells as determined by CFU assay was suppressed over 10-fold in normal populations ( $p = 0.0086$ ), but was not significantly reduced in leukemic cells ( $p = 0.064$ ) (Figure 5B). These data indicate the leukemic stem and progenitor populations in vivo are substantially resistant to radiation-induced damage.

## Discussion

In much the same way that studies of murine hematopoiesis have provided important insights into normal human stem cell biology, we suggest that mouse leukemia models have a similar role in the characterization of human LSC. Our findings extend the work of Dash et al<sup>22</sup> in establishing the mouse as a useful model of blast crisis CML, by providing the first detailed description of LSC in this genetically defined system. With the initial characterization in place, the stage is now set for comprehensive studies to evaluate parameters relevant to the *in vivo* biology of normal vs malignant stem cells. Such efforts will likely take two main forms: 1) studies to better elucidate the mechanisms controlling malignant transformation of stem cells, and 2) studies designed to understand how LSCs can be selectively targeted for destruction. The latter line of investigation represents a particularly formidable challenge, and is complicated by multiple factors. First, the LSC compartment displays a relatively quiescent cell cycle profile, very similar to normal HSC, thus strategies aimed at preferentially active populations are likely to fail. Second, the natural protective mechanisms of stem cells, such as expression of xenobiotic efflux pumps, may be retained by LSC and make them relative difficult to target by at least some drug classes. Third, the ways in which LSC are modulated by the marrow microenvironment (i.e. the stem cell “niche”) are almost entirely uncharacterized. Hence, signals designed to protect normal stem cells from toxic insults may well be operative for LSC. Fourth, as suggested by the radiation experiments in this study, LSC may have enhanced mechanisms of DNA repair and/or the ability to evade senescence induction. Given these and other complicating factors, we suggest that the development and use of genetically and biologically accurate models of *in vivo* leukemogenesis will be essential for the design of better therapeutic regimens.

Findings from the present study suggest that LSC can be effectively modeled in the mouse. Our data indicate the LSC are relatively rare, possess a defined cell surface immunophenotype and cell cycle profile, and display distinct responses to various forms of extrinsic stimuli. All of these features have either been described for human LSC and/or are predicted by previously described components of leukemic disease<sup>9,11</sup>. In addition, our data further corroborate concepts proposed to explain the genesis of LSC. Expression of BCR/ABL provides a direct mitogenic signal, as evidenced by cell cycle analysis of CML

LSC. Intriguingly though, the BCR/ABL-mediated proliferative signal is eclipsed by co-expression of Nup98/HoxA9. Accompanied by an increase in absolute LSC numbers, the activity of Nup98/HoxA9 appears to mediate a switch at the stem cell level from outright proliferative advantage to increased self-renewal as the key pathogenic feature. These findings serve to help explain why co-expression of BCR/ABL+Nup98/HoxA9 is sufficient to induce LSC formation in myeloid progenitor populations (i.e. CMP and GMP), which have typically lost intrinsic self-renewal potential. Moreover, the data are entirely consistent with the work of Jamieson et al in human disease <sup>29</sup>, where CML arises in the stem cell compartment but progression to acute disease can occur in myeloid progenitor populations.

Aside from the primary features mentioned above, several other aspects of the mouse model are worth noting. First, studies of human AML specimens have previously described down-regulation of c-kit as a feature of LSC <sup>34</sup>. Thus, the decreased expression of this common stem cell marker we observe in the mouse model may parallel human disease. Second, studies by Somervaille and Cleary in mouse leukemia models have previously documented relatively promiscuous expression of cell surface markers in amongst primitive cell types <sup>17</sup>. Therefore, finding some degree of leukemia-initiating potential, and/or CFU-potential in multiple compartments is not unprecedented. Indeed, one might imagine that less rigid developmental borders among early cell types may be an intrinsic feature of malignant populations. Third, the effects of both ara-C and imatinib mesylate on normal vs. leukemic stem cells were entirely non-specific, a finding which supports the concept that current therapeutic approaches do not selectively target LSC. Fourth, primitive cells in the bcCML model display a striking degree of radio-resistance. Given the well-documented properties of BCR/ABL in DNA repair <sup>35</sup>, this finding is not surprising, but does represent the first in vivo demonstration that leukemic stem/progenitors are selectively resistant to any form of therapy. If indeed BCR/ABL activity is the key element of this observation, then pretreatment with imatinib prior to radiation should abrogate the protective effect and sensitize LSC to radiation. If true, we suggest this scenario may have relevance for bcCML patients undergoing preparative regimens for BMT.

Going forward there are several lines of investigation to pursue with the mouse LSC model. For example, a variety of other cell surface molecules have been implicated in stem cell biology and should make interesting targets for analysis. Potential niche mediators such as CXCR4, VLA4, VLA5, Tie2, etc. represent molecules that may preferentially modulate the biology of HSC vs. LSC. Indeed, two recent studies indicate that targeting the CD44 antigen may induce LSC-specific loss of function<sup>36,37</sup>. Similarly, sensitivity to therapeutic insult as a function of anatomical location may also be an important avenue to pursue. While HSC appear to reside primarily in the niche, one consequence of transformation may be the ability of LSC to successfully survive in extramedullary sites. If so, then LSC outside the marrow niche to may show increased sensitivity to certain drugs, and thereby suggest that mobilization of primitive leukemic cells could improve responses to at least some forms of therapy.

In summary, with the phenotypic and functional characterization of LSC provided by this and other recent reports using mouse models<sup>15,17,18</sup>, it should be possible to perform detailed in vivo characterization of primitive leukemia cells and developed more selective regimens for selective eradication of malignant stem cells.

## **Acknowledgments**

These studies were supported by grants from the American Cancer Society (RSG-03-096-01-LIB) and U.S. Department of Defense (DAMD17-03-1-0263) to C.T.J., and NIH (R21-CA107355) to A.B. CTJ is a Scholar of the Leukemia and Lymphoma Society.

Contributions: S.J Neering led the laboratory studies. T. Bushell directed all flow cytometry experiments. S. Sozer performed experiments and analyzed data for the CML model. J. Ashton performed radiation sensitivity experiments. R.M. Rossi assisted with numerous animal studies. P.Y. Wang assisted with animal studies. D.R. Bell performed initial studies to establish the bcCML model. D. Heinrich performed Southern blot studies. A. Bottaro designed and analyzed Southern blot studies. C.T. Jordan was the principal investigator.

## References

1. Lapidot T, Sirard C, Vormoor J, et al. A cell initiating human acute myeloid leukaemia after transplantation into SCID mice. *Nature*. 1994;367:645-648.
2. Bonnet D, Dick JE. Human acute myeloid leukemia is organized as a hierarchy that originates from a primitive hematopoietic cell. *NatMed*. 1997;3:730-737.
3. Guan Y, Gerhard B, Hogge DE. Detection, isolation, and stimulation of quiescent primitive leukemic progenitor cells from patients with acute myeloid leukemia (AML). *Blood*. 2003;101:3142-3149.
4. Jordan CT. Unique molecular and cellular features of acute myelogenous leukemia stem cells. *Leukemia*. 2002;16:559-562.
5. Holyoake TL, Jiang X, Drummond MW, Eaves AC, Eaves CJ. Elucidating critical mechanisms of deregulated stem cell turnover in the chronic phase of chronic myeloid leukemia. *Leukemia*. 2002;16:549-558.
6. Reya T, Morrison SJ, Clarke MF, Weissman IL. Stem cells, cancer, and cancer stem cells. *Nature*. 2001;414:105-111.
7. Passegue E, Jamieson CH, Ailles LE, Weissman IL. Normal and leukemic hematopoiesis: are leukemias a stem cell disorder or a reacquisition of stem cell characteristics? *Proc Natl Acad Sci U S A*. 2003;100 Suppl 1:11842-11849.
8. Pardal R, Clarke MF, Morrison SJ. Applying the principles of stem-cell biology to cancer. *Nat Rev Cancer*. 2003;3:895-902.
9. Hope KJ, Jin L, Dick JE. Human acute myeloid leukemia stem cells. *Arch Med Res*. 2003;34:507-514.
10. Jordan CT. Targeting the most critical cells: approaching leukemia therapy as a problem in stem cell biology. *Nat Clin Pract Oncol*. 2005;2:224-225.
11. Guzman ML, Jordan CT. Considerations for targeting malignant stem cells in leukemia. *Cancer Control*. 2004;11:97-104.
12. Al-Hajj M, Becker MW, Wicha M, Weissman I, Clarke MF. Therapeutic implications of cancer stem cells. *Curr Opin Genet Dev*. 2004;14:43-47.
13. Cozzio A, Passegue E, Ayton PM, Karsunky H, Cleary ML, Weissman IL. Similar MLL-associated leukemias arising from self-renewing stem cells and short-lived myeloid progenitors. *Genes Dev*. 2003;17:3029-3035.
14. Huntly BJ, Shigematsu H, Deguchi K, et al. MOZ-TIF2, but not BCR-ABL, confers properties of leukemic stem cells to committed murine hematopoietic progenitors. *Cancer Cell*. 2004;6:587-596.
15. Krivtsov AV, Twomey D, Feng Z, et al. Transformation from committed progenitor to leukaemia stem cell initiated by MLL-AF9. *Nature*. 2006;442:818-822.
16. Huntly BJ, Gilliland DG. Leukaemia stem cells and the evolution of cancer-stem-cell research. *Nat Rev Cancer*. 2005;5:311-321.
17. Somervaille TC, Cleary ML. Identification and characterization of leukemia stem cells in murine MLL-AF9 acute myeloid leukemia. *Cancer Cell*. 2006;10:257-268.
18. Deshpande AJ, Cusan M, Rawat VP, et al. Acute myeloid leukemia is propagated by a leukemic stem cell with lymphoid characteristics in a mouse model of CALM/AF10-positive leukemia. *Cancer Cell*. 2006;10:363-374.
19. Daley GQ, Van Etten RA, Baltimore D. Induction of chronic myelogenous leukemia in mice by the P210bcr/abl gene of the Philadelphia chromosome. *Science*. 1990;247:824-830.
20. Van Etten RA. Models of chronic myeloid leukemia. *Curr Oncol Rep*. 2001;3:228-237.

21. Cuenco GM, Ren R. Cooperation of BCR-ABL and AML1/MDS1/EVI1 in blocking myeloid differentiation and rapid induction of an acute myelogenous leukemia. *Oncogene*. 2001;20:8236-8248.
22. Dash AB, Williams IR, Kutok JL, et al. A murine model of CML blast crisis induced by cooperation between BCR/ABL and NUP98/HOXA9. *Proc Natl Acad Sci U S A*. 2002;99:7622-7627.
23. Mayotte N, Roy DC, Yao J, Kroon E, Sauvageau G. Oncogenic interaction between BCR-ABL and NUP98-HOXA9 demonstrated by the use of an in vitro purging culture system. *Blood*. 2002;100:4177-4184.
24. Yamamoto K, Nakamura Y, Saito K, Furusawa S. Expression of the NUP98/HOXA9 fusion transcript in the blast crisis of Philadelphia chromosome-positive chronic myelogenous leukaemia with t(7;11)(p15;p15). *Br J Haematol*. 2000;109:423-426.
25. Ahuja HG, Popplewell L, Tcheurekdjian L, Slovak ML. NUP98 gene rearrangements and the clonal evolution of chronic myelogenous leukemia. *Genes Chromosomes Cancer*. 2001;30:410-415.
26. Dash A, Gilliland DG. Molecular genetics of acute myeloid leukaemia. *Best Pract Res Clin Haematol*. 2001;14:49-64.
27. Li S, Ilaria RL, Jr., Million RP, Daley GQ, Van Etten RA. The P190, P210, and P230 forms of the BCR/ABL oncogene induce a similar chronic myeloid leukemia-like syndrome in mice but have different lymphoid leukemogenic activity. *J Exp Med*. 1999;189:1399-1412.
28. Kiel MJ, Yilmaz OH, Iwashita T, Yilmaz OH, Terhorst C, Morrison SJ. SLAM family receptors distinguish hematopoietic stem and progenitor cells and reveal endothelial niches for stem cells. *Cell*. 2005;121:1109-1121.
29. Jamieson CH, Ailles LE, Dylla SJ, et al. Granulocyte-macrophage progenitors as candidate leukemic stem cells in blast-crisis CML. *N Engl J Med*. 2004;351:657-667.
30. van Pelt K, de Haan G, Vellenga E, Daenen SM. Administration of low-dose cytarabine results in immediate S-phase arrest and subsequent activation of cell cycling in murine stem cells. *Exp Hematol*. 2005;33:226-231.
31. Graham SM, Jorgensen HG, Allan E, et al. Primitive, quiescent, Philadelphia-positive stem cells from patients with chronic myeloid leukemia are insensitive to STI571 in vitro. *Blood*. 2002;99:319-325.
32. Meng A, Wang Y, Brown SA, Van Zant G, Zhou D. Ionizing radiation and busulfan inhibit murine bone marrow cell hematopoietic function via apoptosis-dependent and -independent mechanisms. *Exp Hematol*. 2003;31:1348-1356.
33. Wang Y, Schulte BA, Larue AC, Ogawa M, Zhou D. Total body irradiation selectively induces murine hematopoietic stem cell senescence. *Blood*. 2005.
34. Blair A, Sutherland HJ. Primitive acute myeloid leukemia cells with long-term proliferative ability in vitro and in vivo lack surface expression of c-kit (CD117). *Exp Hematol*. 2000;28:660-671.
35. Skorski T. BCR/ABL regulates response to DNA damage: the role in resistance to genotoxic treatment and in genomic instability. *Oncogene*. 2002;21:8591-8604.
36. Krause DS, Lazarides K, von Andrian UH, Van Etten RA. Requirement for CD44 in homing and engraftment of BCR-ABL-expressing leukemic stem cells. *Nat Med*. 2006;12:1175-1180.
37. Jin L, Hope KJ, Zhai Q, Smadja-Joffe F, Dick JE. Targeting of CD44 eradicates human acute myeloid leukemic stem cells. *Nat Med*. 2006;12:1167-1174.

**Table 1: Lineage analysis of normal vs. leukemic populations**

Population	Naïve ctrl	GFP ctrl		BCR		BCR+Nup	
		GFP+	GFP-	GFP+	GFP-	GFP+/YFP+	GFP-/YFP-
B cells	30%	47%	21%	37%	16%	15%	13%
T cells	14%	8%	21%	10%	14%	6%	18%
RBC	9%	7%	20%	6%	12%	1%	15%
Myeloid	36%	28%	31%	34%	46%	46%	43%
Lin-	11%	<b>10%</b>	6%	<b>12%</b>	12%	<b>32%</b>	11%

GFP ctrl = animals transplanted with cells infected with the GFP control retrovirus

BCR = animals transplanted with cells infected with the BCR/ABL retrovirus

BCR+Nup = animals transplanted with cells infected with the BCR/ABL and Nup98/HoxA9 retroviruses.

GFP+ = indicates percentage of indicated lineage within GFP+ (i.e. infected) bone marrow cells

GFP- = indicates percentage of indicated lineage within GFP- (i.e. non-infected) bone marrow cells

**Table 2: CFU frequency for sorted subpopulations**

<u>Cells</u>	<u>Fraction</u>	<u>CFU/5000 cells</u>
Naïve BM	Total MNC	10 +/- 2
	Lin-	101 +/- 30
	Lin-/Kit+/Sca-	256 +/- 60
	Lin-/Kit+/Sca+	1800 +/- 372
CML BM (GFP+)	Total MNC	9 +/- 3
	Lin-	69 +/- 19
	Lin-/Kit+/Sca-	104 +/- 37
	Lin-/Kit+/Sca+	1743 +/- 314
bcCML BM (GFP+/YFP+)	Lin+	20 +/- 5
	Lin-/Sca-/CD150+	1575 +/- 525
	Lin-/Sca-/CD150-	3300 +/- 1100
	Lin-/Flt3-/Fc-low/CD150+	1750 +/- 585
	Lin-/Flt3-/Fc-low/CD150-	2210 +/- 735
	Lin-/Sca+/Flt+/CD150-	2395 +/- 800

Naïve BM = bone marrow from naïve control animals.

CML BM = bone marrow from animals bearing BCR/ABL transduced cells.

bcCML BM = bone marrow from animals bearing BCR/ABL + Nup98/HoxA9 transduced cells.

CFU/5000 = number of colony-forming units (+/- std deviation) normalized to 5000 cells.

**Table 3: Stem and progenitor cell analyses of frequency and cell cycle status**

BM Source	subpopul.	Stem Cells			Progenitors			
		Phenotype	Frequency	Cycle %	Phenotype	Frequency	Cycle %	CFU/25K
Naïve control	n.a.	Sca+/Kit+/Lin-	0.08%	10%	Kit+/Lin-	1.70%	27%	30
GFP control	GFP+	Sca+/Kit+/Lin-	0.02%	14%	Kit+/Lin-	1.50%	35%	
	GFP-	Sca+/Kit+/Lin-	0.03%	14%	Kit+/Lin-	1.90%	34%	
BCR only	GFP+	Sca+/Kit+/Lin-	<b>0.02%</b>	<b>32%</b>	Kit+/Lin-	<b>1.90%</b>	43%	<b>48</b>
	GFP-	Sca+/Kit+/Lin-	0.04%	<b>17%</b>	Kit+/Lin-	1.60%	25%	
BCR + Nup	GFP+	Sca+/Flt+/Lin-*	<b>0.30%</b>	<b>10%</b>	Kit+/Lin-	<b>8.40%</b>	28%	<b>442</b>
	GFP-	Sca+/Kit+/Lin-	0.07	<b>13%</b>	Kit+/Lin-	1.90%	21%	

Freq. = percentage of stem or progenitors cells as defined by the indicated phenotype.

Cycle% = percentage of cells in S + G2 phase of cell cycle.

CFU/25K = number of colony-forming units per 25,000 cells plated in methylcellulose assay.

\* = LSC phenotype (Sca+, Flt3+, kit-lo, CD34+, CD150-)

**Table 4: Cell cycle analyses of stem and progenitor cells after drug challenge**

	<u>Stem Cells*</u>		<u>Progenitors*</u>	
	Normal	bcCML	Normal	bcCML
Untreated	19%	18%	27%	29%
Ara-C 4 hr	12%	11%	12%	17%
Ara-C 20 hr	18%	23%	21%	29%
Imatinib	13%	14%	35%	36%

\*Percentage of cells in S+G2 phases of cell cycle for indicated populations. Analyses performed in triplicate for each condition, all results within 10% standard deviation.

## Figure Legends

Figure 1: Characterization of leukemia models

A) Example of bone marrow derived from a primary recipient of co-infected cells. The BCR/ABL transduced cells are detected by GFP expression and the Nup98/HoxA9 infected cells are detected by YFP expression. Panels I and II indicate singly infected populations, whereas panel III shows cells that are successfully transduced with both the BCR/ABL and Nup98/HoxA9 vectors. B) Analysis of host origin for GFP-/YFP- cells from a secondary recipient is shown in order to establish that potential donor leukemic cells have not lost GFP/YFP expression. Fidelity of the system is demonstrated by greater than 99% purity of the host marker (Ly5.2).

Figure 2: Kaplan-Meier analysis of survival for CML and bcCML models

A) Donor populations of purified HSC, CMP, or GMP were infected with the BCR/ABL retrovirus and transplanted into primary mice. B) Donor populations of purified HSC, CMP, or GMP were infected with the BCR/ABL + Nup98/HoxA9 retroviruses and transplanted into primary mice. Numbers of recipients indicated in parentheses for each donor cell type. Days of survival post-transplant are indicated for each cell type on the X-axis.

Figure 3: Southern blot analysis of bcCML

Bone marrow DNA from five primary recipient mice (left panel) was digested with EcoRI and hybridized with a GFP probe, which detects bands of unique size for each independent viral integrant. For primary animals #2, 3, and 4, three secondary recipients (a, b, and c) were established. The right panel shows EcoRI digestion and GFP probe analysis of the secondary recipients in comparison to each primary donor.

Figure 4: Phenotypic analysis of normal vs. leukemic stem cell populations

Examples of stem cell phenotyping are shown for GFP control (upper left), CML (upper right), and bcCML (bottom panels) populations. In each case, cells were first gated on the Lin<sup>-</sup> population. GFP and CML populations show typical labeling for stem cell markers c-kit and sca-1. Labeling of bcCML shows reduced c-kit expression (lower left). The CD150 negative and Flt3 bright subpopulation of bcCML cells (lower right) is highly enriched for LSC (1 in 7 cells by limiting dilution).

Figure 5: Phenotypic and in vitro analyses of irradiated normal vs. leukemic animals

A) Bone marrow cells were isolated from control vs. irradiated animals and labeled with antibodies to detect stem cell populations (indicated by the box in each panel). The top panels show GFP<sup>-</sup> (i.e. normal) cells and the bottom panels show GFP<sup>+</sup> (i.e. leukemic) cells. The data shown for each panel are gated on the Lin<sup>-</sup> population. B) Colony-forming units (CFU) were determined for sorted GFP<sup>+</sup> (leukemic) and GFP<sup>-</sup> (normal) populations. Data shown are the absolute number of colonies measured per 5000 cells plated (triplicate assays). Asterisk (\*) indicates statistical significance ( $p = 0.0086$ ) as determined by Student t test.

Figure 1

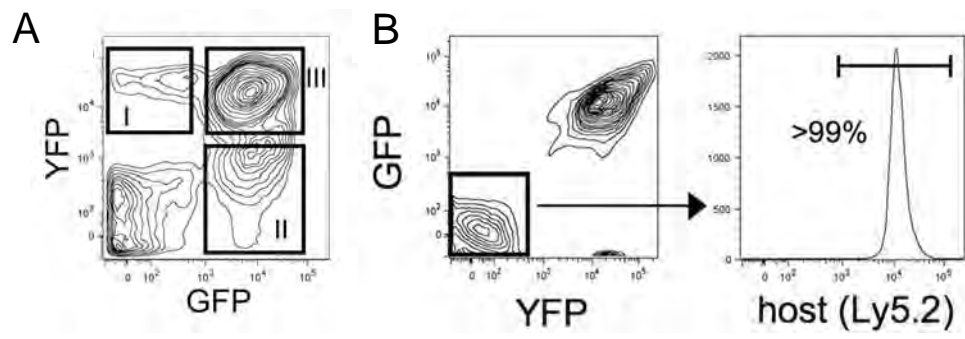


Figure 2

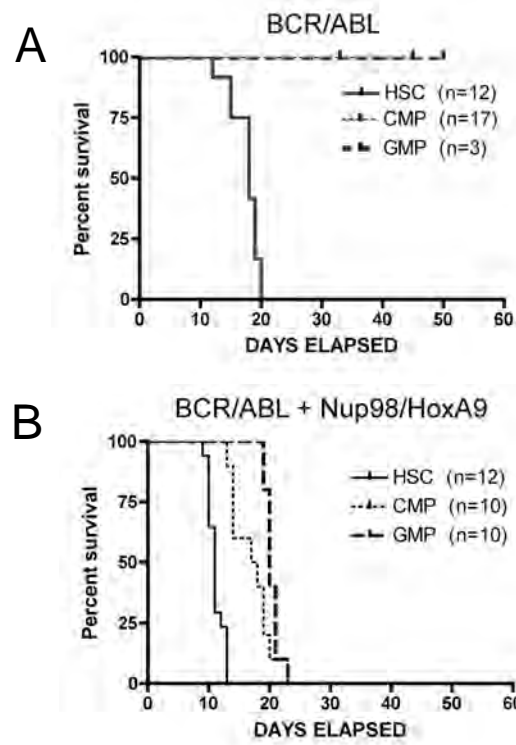


Figure 3

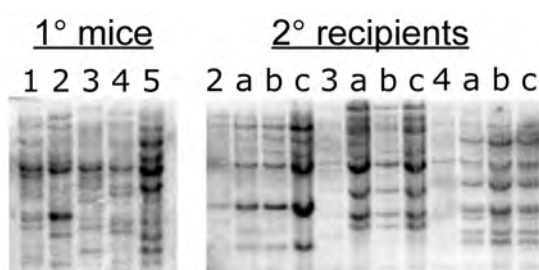


Figure 4

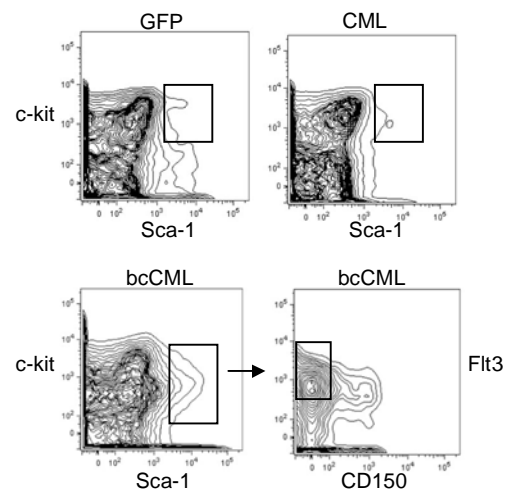


Figure 5

